Elsevier Editorial System(tm) for Journal of Volcanology and Geothermal Research
Manuscript Draft

Manuscript Number: VOLGEO5127R1

Title: Origin and evolution of silicic magmas at ocean islands: Perspectives from a zoned fall deposit on Ascension Island, South Atlantic

Article Type: Research paper

Keywords: Ascension Island; magma evolution; zonation; magma chamber processes; fractionation

Corresponding Author: Dr. Katy Jane Chamberlain, Ph.D.

Corresponding Author's Institution: Durham University

First Author: Katy Jane Chamberlain, Ph.D.

Order of Authors: Katy Jane Chamberlain, Ph.D.; Jenni Barclay; Katie J Preece; Richard J Brown; Jon P Davidson; E IMF

Abstract: Ascension Island, in the south Atlantic is a composite ocean island volcano with a wide variety of eruptive styles and magmatic compositions evident in its ~1 million year subaerial history. In this paper, new observations of a unique zoned fall deposit on the island are presented; the deposit gradationally changes from trachytic pumice at the base, through to trachy-basaltic andesite at the top of the deposit. The key features of the eruptive deposits are described and are coupled with whole rock XRF data, major and trace element analyses of phenocrysts, groundmass glass and melt inclusions from samples of the compositionally-zoned fall deposit to analyse the processes leading up to and driving the explosive eruption. Closed system crystal fractionation is the dominant control on compositional zonation, with the fractionating assemblage dominated by plagioclase feldspar and olivine. This fractionation from the trachy-basaltic andesite magma occurred at pressures of ~ 250 MPa. There is no evidence for multiple stages of evolution involving changing magmatic conditions or the addition of new magmatic pulses preserved within the crystal cargo. Volatile concentrations range from 0.5 to 4.0 wt.% H2O and progressively increase in the more evolved units, suggesting crystal fractionation concentrated volatiles into the melt phase, eventually causing internal overpressure of the system and eruption of the single compositionally-zoned magma body. Melt inclusion data combined with Fe-Ti oxide modelling suggests that the oxygen fugacity of Ascension Island magmas is not affected by degree of evolution, which concentrates H2O into the liquid phase, and thus the two systems are decoupled on Ascension, similar to that observed in Iceland. This detailed study of the zoned fall deposit on Ascension Island highlights the relatively closed-system evolution of felsic magmas at Ascension Island, in contrast to many other ocean islands, such as Tenerife and Iceland.

Dr. Margaret T. Mangan,
Editor, Journal of Volcanology and Geothermal Research,
U.S. Geological Survey,
Menlo Park,
California, USA

August 3rd 2016

Dear Dr. Mangan,

This letter is to accompany a revised version of our manuscript ID VOLGEO5127: " Origin and evolution of silicic magmas at ocean islands: Perspectives from a zoned fall deposit on Ascension Island, South Atlantic". Many thanks to you and the reviewers for your work on the manuscript. The comments of the two reviewers are copied below in blue italics, while our responses are in black.

We hope you find that these changes are acceptable, and that you feel able to accept the revised manuscript for publication. Should you require any further information or clarification, please let me know.

Best wishes

Katy Chamberlain
On behalf of the authors

Responses to reviewer comments. All line numbers refer to those in the commented version of the manuscript online.

Reviewer #1 comments

RESULTS

1) Petrography: I suggest to discuss in more detail the petrography of the studied samples. At line 31 the authors state: "Crystal phases are always unzoned in back-scattered electron (BSE) imagery (Fig. 6), and all crystal phases are euhedral with no evidence for any dissolution having occurred. Olivine is typically melt inclusion-rich, with multiple melt inclusions per crystal." Observing the Fig.6, it seems that the olivine shows evidence of resorption. Please discuss in more detail the petrography of the samples, not only the evidence that supports the proposed conclusions.

We have now tried to describe the petrography of the samples as fully as we can, and have added more details where appropriate. However, we cannot undertake a detailed petrographic analysis of percentages of crystal phases. The pumice and scoria contain < 5% of crystals, thus given the number of crystals in any one section, it would be difficult to get representative crystal percentages.

We disagree that the crystals show evidence for resorption. This conclusion might be drawn because we have shown 2D BSE images of the crystals. In 3D crystals which have these embayed inclusions, there are euhedral crystal faces on other sides- not supporting resorption as the cause of this structure. All crystal phases imaged under BSE show no evidence for zonation, and are all euhedral. This comes from our crystal concentration and separation and thus we are confident we have sampled a representative proportion. We have now made this clearer in the text.

2) Chemical analyses of melt inclusions/matrix glass: The authors have a lot of trace element data in the supplementary material. Please discuss, plot and model these data to support the proposed conclusions. I would like to see at least some REE and incompatible PM normalized spider diagrams and a quantitative modeling based on trace elements of the melt/matrix phases and whole rocks.

This is a good point and we have now added a fifth panel to figure 8 to show the primitive mantle normalized variation in trace elements for the three identified subunits. However , as the plot shows there is not a great deal of variation between the subunits and we have discussed the most significant elemental variation in the text. Figure 10 now shows the results from fractional crystallization modeling.

3) Isotopes: the addition of isotopic data will help to support or discard the hypothesis of a closed system behavior proposed by the authors. Also, it will improve the currency of the manuscript.

There are detailed studies of Ascension Island isotopic data, carried out by many authors (Kar et al., 1998; Weaver et al., 1996; Kar PhD thesis; Paulick et al., 2010). However, these show little evidence to suggest that surrounding country rock (which is young oceanic crust, of similar isotopic composition to the basalt erupted on Ascension) would have significantly different isotopic composition (given that no mixing with country rock has been previously identified) to impart any evidence for mixing and/or assimilation isotopically. We have therefore not collected isotopic data for these sub-units as we feel the origins of the zoned fall are best explored looking at the mineral specific and glass data.

4) Magmatic conditions: "Given the commonly cited uncertainties of ± 30 °C associated with FeTi-oxide thermometry (e.g. Blundy & Cashman, 2008) these results indicate little evidence for a thermal gradient existing within the magmatic system in the months to weeks prior to eruption." If the error is +/- 30, there is no difference between 845° and 866°C. Please discuss.

Yes, this is why we say there is little evidence for a thermal gradient in the magma chamber shortly pre-eruption (and hence no internal driver for convection, see point below). We have amended the text to make sure this interpretation is clearer.

5) Pressure: Finding a 'constant' entrapment pressure of ca. 250 MPa (8 km) could also mean that the inclusions have been re-homogenized at that pressure after a complex history. Please discuss.

In fact we do not find a ‘constant’ entrapment pressure, and have corrected the text to highlight this, and point towards figure 9 that shows the range. This range is interpreted to reflect partial re-homogenization upon ascent. It is true however, that the maximum entrapment pressure from each subunit of the fall deposit, is relatively constant, within uncertainty. There is no evidence in the crystal compositions to suggest a complex history, with transport from multiple storage regions and/or magma mixing, hence we believe our handling of the data to yield the most insights into the evolution of the zoned fall. We have edited the text to make this as clear as possible on page 10 and 11.

DISCUSSION

1) Final stratification: What about of a complex history with only the last part of the history in agreement with the ideas proposed in the present manuscript? Please discuss all the potential hypothesis for the origin and the evolution of the plumbing

system.

We have no evidence for any complex history of the magmas, as discussed in the final stratification paragraph. While there could be multiple magmatic sources, and mixing occurring, this all happened prior to crystal growth, as crystals show no zonation, melt inclusion compositions closely mirror matrix glass compositions, and entrapment pressures suggest no differences depth of melt inclusion entrapment within the whole unit. Therefore, while there is every possibility of a more complex history, we so no evidence of this in the crystals, melt inclusions, and matrix glass studied here, and therefore we have no evidence for any prior history. We have added text to highlight that we are only able to probe the history of the magma since crystal growth began, and have tried to highlight that we cannot see into the 'melt-only' history of this magma. Further discussion of what may have occurred prior to crystal growth would be purely speculative, and thus we have avoided this to any significant degree.

2) The role of fractional crystallization: Why the authors only model the major elements? If the proposed model is correct, it should work for major elements, trace elements, and isotopes. Please provide a comprehensive modeling of the system.

We do not think that isotopic data would add significant value to this paper given the lack of variation in isotopes across the island (see above). We have not modeled trace elements in the fractional crystallization as there is relatively little variance and we feel that the choice of distribution coefficient for trace elements in a sub-alkaline system, will significantly affect the results of this modeling, and introduce significant uncertainties. Qualitatively the trace elements expected to be sensitive to fractional crystallisation show trends consistent with the major elements and there are no other variations that would suggest that an alternative explanation might be valid, thus in this instance, major element modeling is the most robust way to show the effects of fractional crystallization. However, the addition of figure 10 demonstrates the role of fractional crystallization and now shows the process more clearly.

3) Convection in a stratified magma body: "It seems likely that no chamber-wide convection was occurring due to reasons discussed above". I do not agree. Convection could act for a while then stop allowing for a stratification.

There is no evidence for any initial homogenization from convection, while it could have operated for a time- we see nothing to support this conjecture. We have clarified the text to highlight that the crystals only show evidence for stratification, and therefore at the time of crystal growth we see no evidence for convection occurring.

4) Eruptive triggers: the presented data do not support the proposed discussion. A water content of 4% wt. does not imply that the eruption "was triggered by internal overpressure due to fractionation increasing the concentration of magmatic volatiles in the magma." Of course, we cannot exclude that hypothesis, but the authors do not show any evidence of it.

We discuss other alternative triggering mechanisms, such as mixing of magmas, tectonic triggering, but do not see evidence for this in the compositionally-zoned fall (or on Ascension Island, in general)- and hence suggest that the higher water contents, concentrated during fractionation, caused an internal over pressure of the system. There is no evidence for any external trigger. While it is indeed hard to prove that internal overpressure was a trigger for the compositionally zoned fall, we think that the lack of evidence for any other trigger supports this hypothesis. We have altered

the text to highlight that this is trigger mechanism is an inference from our data, rather than a definite cause of eruption.

5) Please rearrange the conclusions in the light of the provided comments.
We have added extra text in our conclusions based on the comments of this reviewer.

Reviewer #2 comments:

Abstract, line 15-16: "Volatile concentrations are high (~4 wt.% H2O) is misleading for two reasons: 1) most of the un-degassed melt inclusions have 2-4 wt.% H2O. The max is 4 wt.%. 2) 4 wt.% H2O is not that high. See Plank et al 2013, EPSL, "Why do all mafic arc magmas contain 4 wt% water on average?"). Sentence should say, "Volatile concentrations range from 0.5 to 4.0 wt.% H2O and progressively increase in the more evolved units, suggesting crystal fractionation concentrated volatiles into the melt phase…."
Corrected.

Abstract end: Another interesting finding of this study is that they see evidence for decoupling of the H2O and fO2 systematics at Ascension Island, similar to what is observed at Hekla volcano, Iceland. Conclusion point #4 highlights this result, but it is not mentioned in the abstract. The authors should add one more sentence to the end of the abstract to highlight this finding.
We have added an extra sentence in the abstract to highlight this finding.

Page 3, line 14: should add citation to Pallister et al., 1992 Nature
Added, and added in the reference list.

Page 5, line 15: rewrite to say ", and feldspar is the only identifiable phase in hand sample."
Corrected.

Page 6, line 26: the word "reduce" is not needed 3 times in this sentence. Just use it once and then list all the items that have been reduced.
Corrected.

Page 6, lines 29: Is 24Mg2+ being resolved from 2 x 12C+?
Yes. This was already described in our methods section, so have left text as is.

Figure 2: the color scheme does not match the descriptions in (b). Although it is explained in the figure caption that lithic clasts are brown and scoria is dark gray, it would make more sense to have the scoria be brown as this is the color in the photo and description. I was confused when I read the descriptions and it said that subunit B had the first appearance of brown scoria, but the brown unit is present in all the subunits. This confusion is eliminated by changing the scoria to brown.
This has been changed in the figure and caption, so that the scoria is now brown, and the lithics are black.

Figure 9: If the text is going to say 240 MPa max, then the histograms should be broken down into 20 MPa bins to show that the maximum is 240 MPa not 250 MPa.

240 MPa corresponds to ~8km, which is the base of the oceanic crust in this setting. This is a logical place for magma to stall. It is odd that the authors make no mention of the significance of this depth/location. Something should be added on page 10 and potentially in the abstract and conclusions.

We have not corrected the figure, as the 240 MPa is a mistake; we have corrected this to 250MPa. We have also added text to highlight the significance of the pressure corresponding to the base of the crust.

If the fractional crystallization modelling be summarized into one figure (it can be), I think it would be a nice addition to the paper. Having to delve through the electronic supplement to find this stuff is a pain. Just add a new figure 10 to illustrate the results of the modelling.

A new figure has been made with major element data from matrix glass plus representative crystal phases; to demonstrate the fractionation occurring.

Brian Jicha
University of Wisconsin-Madison

Highlights

Origin and evolution of silicic magmas at ocean islands: Perspectives from a zoned fall deposit on Ascension Island, South Atlantic (Chamberlain et al.)

- Deposit originates from a single compositionally zoned magma chamber at ~250 MPa
- Zonation created by closed-system fractional crystallisation of olivine + feldspar
- Eruption triggered by internal overpressure from increasing volatile concentrations

Origin and evolution of silicic magmas at ocean islands: Perspectives from a zoned fall deposit on Ascension Island, South Atlantic

K. J. CHAMBERLAIN[1*], J. BARCLAY[2], K. PREECE[2], R. J. BROWN[1], J. P. DAVIDSON[1], EIMF[3]

[1] DEPARTMENT OF EARTH SCIENCES, UNIVERSITY OF DURHAM, DURHAM, DH1 3LE, UK
[2] SCHOOL OF ENVIRONMENTAL SCIENCES, UNIVERSITY OF EAST ANGLIA, NORWICH, NR4 7TJ, UK
3 EDINBURGH ION MICROPROBE FACILITY, UNIVERSITY OF EDINBURGH, EDINBURGH,

Manuscript for: *Journal of Volcanology and Geothermal Research*

Running title: Zoned Ascension fall units

Keywords: Ascension Island, magma evolution, zonation, magma chamber processes, fractionation, closed-system

Revised Version~~: 4~~; 3~~11~~rd~~th~~ August~~May~~ 2016

*Corresponding author. Phone (+44) 191 334 2300, Fax (+44) 191 334 2301
Email addresses: ~~katy.chamberlain@durham.ac.uk~~katyjanechamberlain@gmail.com

ABSTRACT

Ascension Island, in the south Atlantic is a composite ocean island volcano with a wide variety of eruptive styles and magmatic compositions evident in its ~1 million year subaerial history. In this paper, new observations of a unique zoned fall deposit on the island are presented; the deposit gradationally changes from trachytic pumice at the base, through to trachy-basaltic andesite at the top of the deposit. The key features of the eruptive deposits are described and are coupled with whole rock XRF data, major and trace element analyses of phenocrysts, groundmass glass and melt inclusions from samples of the compositionally-zoned fall deposit to analyse the processes leading up to and driving the explosive eruption. Closed system crystal fractionation is the dominant control on compositional zonation, with the fractionating assemblage dominated by plagioclase feldspar and olivine. This fractionation from the trachy-basaltic andesite magma occurred at pressures of ~ 2540 MPa. There is no evidence for multiple stages of evolution involving changing magmatic conditions or the addition of new magmatic pulses preserved within the crystal cargo. Volatile concentrations range from 0.5 to 4.0 wt.% H_2O and progressively increase in the more evolved units, suggesting crystal fractionation concentrated volatiles into the~~are high (~ 4 wt.% H_2O) suggesting that progressive crystal fractionation concentrated volatiles into the~~ melt phase, eventually causing internal overpressure of the system and eruption of the single compositionally-zoned magma body. Melt inclusion data combined with Fe–Ti oxide modelling suggests that the oxygen fugacity of Ascension Island magmas is not affected by degree of evolution, which concentrates H_2O into the liquid phase, and thus the two systems are decoupled on Ascension, similar to that observed in Iceland. This detailed study of the ~~compositionally~~ zoned fall deposit on Ascension Island highlights the relatively closed-system evolution of felsic magmas at Ascension Island, in contrast to many other ocean islands, such as Tenerife and Iceland.

Formatted: Subscript

Formatted: Subscript

INTRODUCTION

Ascension Island, in the south Atlantic, is a 12 km diameter ocean island volcano located 90 km west of the mid Atlantic Ridge (MAR). It is similar to Iceland and many other ocean island volcanoes in having a ~~relatively high~~significant proportion of silicic volcanic products preserved at the surface (~14% of the surface exposure, Nielson & Sibbett, 1996, compared with ~10% surface area in Iceland, Walker, 1966, Carley et al., 2011). Understanding the processes responsible for the production of silicic magmas at ocean islands is important not only for our present understanding of magmatic processes and magmatic

evolution, but also provides critical insights into the mechanisms behind the generation of the first continental crust in the Archean (e.g. Gazel et al., 2014; Mancini et al., 2015). Two main methods have been proposed for the generation of evolved melts in thin oceanic crust: (i) low-degree partial melting of hydrothermally-altered crust to produce primary silicic melt (e.g. Sverrisdottir, 2007; Carley et al., 2011; Kuritani et al., 2011) or (ii) fractionation (in potentially multiple stages) from a basaltic parental magma (e.g. Watanabe et al., 2006; Snyder et al., 2007; Mortensen et al., 2009; Mancini et al., 2015), or some combination of these processes.

Zoned volcanic deposits preserve the moment in magmatic evolution when ~~disparate~~ distinct magmas are ~~brought~~ erupted together, and might only be observable through disequilibria in phenocryst assemblages in otherwise homogeneous deposits. They can provide a direct record of processes responsible for magmatic evolution (and timescales over which they occur), such as fractionation, mixing and assimilation (e.g. Watanabe et al., 2006; Snyder et al., 2007; Sverrisdottir, 2007; Mortensen et al., 2009; Carley et al., 2011; Kuritani et al., 2011; Mancini et al., 2015).

Zoned volcanic deposits may also yield insights into the processes responsible for eruptive triggering (e.g. Sverrisdottir, 2007; Kuritani et al., 2011). Recharge of volcanic systems (potentially preserved as two magmatic types in zoned volcanic deposits) has often been cited as a trigger for eruptions (e.g. Sparks and Sigurdsson 1977; Pallister et al., 1992; Sverisdottir, 2007; Saunders et al., 2012; Sliwinski et al., 2015) whether due to a direct increase in volume, causing failure of the magma chamber wall rocks (e.g. Jellinek and DePaolo 2003), the buoyancy-driven effects of accumulating magma (e.g. Carrichi et al., 2014; Malfait et al., 2014), or by indirectly causing changes in volume of saturated gases and crystal cargo (e.g. Snyder 2000). However, other eruptive triggers are well-documented, including tectonic triggers from earthquake activity (e.g. Allan et al., 2012), changing crustal stress-states (e.g. Bonali et al., 2013) and internal overpressure from crystal fractionation driving increased volatile concentrations in the remaining magma (e.g. Stock et al., 2016).

Here we present field observations, whole rock major and trace element data, mineral compositions and melt inclusion analyses from a unique zoned fall deposit on Ascension Island, to understand the processes responsible for silicic melt generation, evolution and eruption in young (<7 Ma) oceanic crust on Ascension Island. The zoned fall deposit is unique on Ascension Island in that it changes gradationally from trachytic pumice at the base of the unit, to a trachy-basaltic andesite scoria at the top of the unit, with no textural evidence for mingling between pumice and scoria. We use this deposit to probe the origins of felsic

melt at Ascension Island, to understand how the zonation is produced, and by inference what may have triggered the eruption. In particular, we use this deposit to test whether the zonation is the result of two distinct magma batches partially homogenizing (open system), if it is generated via *in situ* fractionation (closed system), or if it is the result of a combination of multiple processes.

GEOLOGICAL SETTING

Ascension Island (7° 56' S; 14° 22' W) is located in the southern Atlantic Ocean, 90 km west of the Mid-Atlantic Ridge and 50 km south of the Ascension Fracture Zone (AFZ; Fig. 1). Volcanism has been present at Ascension for ~ 6 – 7 Myr and the subaerial portion of the island (only 1% of the total ~3800 km^3 edifice, Harris, 1983) was formed in the last ~1 Myr (Weaver et al., 1996; Jicha et al., 2014). Volcanic deposits on Ascension are widely variable, with lava flows, lava domes, pyroclastic fall units, pyroclastic flow units (Daly, 1925; Harris, 1983; Weaver et al., 1996; Hobson, 2001).

Subaerial volcanism has been the product of a transitional to mildly alkali magmatic series of olivine basalt – hawaiite – mugearite – benmoreite – trachyte – rhyolite. Previous investigations into Ascension Island volcanism have focussed on the geochemical distinctions between magmas; mafic volcanic products have been split into three main categories, based on their Zr/Nb ratios, which has been inferred to represent varying source characteristics underlying Ascension. Mafic volcanic products occur ~~all~~ across all of ~~of~~ Ascension, but felsic volcanic products are more localised and outcrop in two main areas of the island: a 'Central Felsic Complex', which contains Green Mountain, the highest point on the island at 859m asl, (see Fig. 1; Kar et al., 1998) and the younger 'Eastern Felsic Complex' (Fig. 1; Kar et al., 1998; Hobson, 2001; Jicha et al., 2014). Previous studies have suggested that the felsic magmas are a product of fractional crystallisation from the high Zr/Nb basalt (Weaver et al., 1996; Kar et al., 1998), with limited evidence for interaction between magma batches (Kar et al., 1998).

THE COMPOSITIONALLY ZONED FALL

The compositionally-zoned fall unit (Fig. 2) is found in multiple locations across the island (Fig. 3) although ~~this~~ it is dominantly found in the Eastern Complex (Fig. 1). Along the North East coast the compositionally-zoned fall outcrops below a (geochemically un-related) voluminous trachyte flow at NE Bay, which has a $^{40}Ar/^{39}Ar$ date of 169 ka (±43 ka [2σ],

Jicha et al., 2014). Thus the eruption responsible for the deposition of the compositionally-zoned fall is also likely comparatively young.

The vent for the compositionally-zoned fall deposit was identified by the coarsening characteristics of the multiple exposures (see Fig. 3 for maximum lithic clast and thickness variations at every outcrop observed), and by the presence of a fissure through an underlying mafic lava flow, overlain by the coarsest and thickest deposits of the compositionally-zoned fall on the island. At this locality the bombs of pumice are up to 30 cm in diameter, and lithic clasts (of trachyte lava and dense mafic lava and scoria) are up to 15 cm in diameter. The limited outcrops indicate dispersal towards the north east, which is consistent with the dominant south-westerly wind direction at Ascension (see Fig. 3).

For the purposes of systematic sampling, three distinct subunits were delineated (Figs. 2, 3). The lowermost subunit (A) consists of felsic cream to light brown coloured pumice which is variably oxidised to orange and purple colours in the centre of clasts, and ~15% lithic clasts. Juvenile pumice is crystal poor, with <5% crystals which include feldspar and olivine. Crystals are always <1 mm in diameter. Lithic clasts present include green trachyte lava and mafic lava (oxidised to red and unoxidised black). Subunit B marks the first appearance of the transitional brown pumice-scoria with a coarser vesicularity than that of the light brown pumice (Fig. 4). The change from cream pumice to brown pumice-scoria is gradational, with transitional light brown pumice-scoria clasts identified, implying that the change in colour is both textural and compositional in origin. Lithic clasts comprise ~15% of this unit, and are dense mafic lavas (red and black) and minor green trachyte lavas. Juvenile pumice-scoria is crystal poor with <5% macrocrysts, and ~~only~~ feldspar is the only identifiable phase in hand sample. Subunit C marks the change to less than 15% pumice in the unit (gradational), and the juvenile material is dominated by dark brown scoriacious clasts. Lithic clasts are now ~10% and consist of dense mafic lavas (oxidised and unoxidised). The scoria has a very coarse vesicularity, with vesicles up to cm-scale (Fig. 4).

The compositionally-zoned fall deposit is most easily recognised by the systematic zonation of cream pumice clasts (subunit A) passing upwards into brown pumice-scoria (subunit B) to dark brown scoria (subunit C; Fig. 2). The compositionally-zoned fall unit varies in thickness from ~50 cm in the central areas of the island, to more than 10 m adjacent to the vent (see Fig. 3). The deposit generally has a fine-grained base, which coarsens upwards to the centre of the subunit A (Fig. 2), with the coarsest juvenile clasts in the lowermost 20-50% of subunit A (Fig. 2), indicating that the eruption reached its maximum energy output prior to the eruption of less-evolved magma.

SAMPLING AND ANALYTICAL TECHNIQUES

Bulk samples were collected from the three subunits of the zoned fall deposit (Fig. 2). Samples were sieved to >8mm or >16mm to ensure than any lithic clasts could be identified and removed by hand. Samples were collected from multiple localities and analysed for whole rock major and trace elements (Fig. 3). One locality (Fig. 3) was sampled more intensively than the three major subunits to understand in more details the nature of the zonation in the fall deposit (see Table 1 for sampling details).

Any adhering matrix or oxidised rind was removed by hand, and samples were then soaked in (frequently changed) milli-RO water for a minimum of one week. Samples were then dried thoroughly at 60 °C prior to crushing. An aliquot of the sample was selected to mill for X-ray fluorescence (XRF) analysis at the University of East Anglia (UEA) using a Brucker-AXS S4 Pioneer. The remainder of the sample was crushed by hand, before being sieved into various size fractions (< 2 mm). Crystals and glass separates were hand-picked from the 0.5 – 1 mm size fraction, mounted into low-activity epoxy discs, and polished to expose melt inclusions and crystal cores. Melt inclusion-bearing crystals were imaged using reflected light microscopy prior to analysis. Secondary ion mass spectrometry (SIMS) measurements of selected volatile and trace elements were made prior to measurement of other major and trace elements by electron probe microanalysis (EPMA) and laser ablation inductively coupled plasma mass spectrometry (LA-ICPMS), following the method of Humphreys et al. (2006).

Mounts of melt-inclusion bearing crystals were gold-coated and analysed using secondary ion mass spectrometry (SIMS) for isotopes of volatile ($^{1}H^{+}$ and $^{12}C^{+}$) and key trace elements (Li, B, Be, F, S, Cl, Rb, Sr, Zr, Nb, Ba) using a Cameca 1270 ion microprobe at the NERC Ion Microprobe Facility at the University of Edinburgh (UK). During analysis, the primary beam was rastered for 180 seconds over an area of about 35 μm^2 prior to data acquisition to remove the gold coat and any possible surface contamination. Secondary ions were then sputtered from melt inclusions with a 5-6 nA primary $^{16}O_2^-$ beam focused to a ~25×35 µm spot. The area analysed was reduced using a (field) aperture to accept on the central 20 μm^2 of the bombarded area. Analyses were done in two parts; initially volatiles H, C, F, S, and Cl (plus majors Mg^{2+} and Si) followed by traces Li, Be, B, Rb, Sr, Zr, Nb and Ba (plus majors Mg and Si) in the same hole. Energy filtering (75±20 eV) was employed to reduce the molecular ion presence, ~~reduce~~ the ratio susceptibility to charging effects and-

~~reduce~~ any potential matrix effects. The mass resolution employed (M/ΔM>2500) was sufficient to fully resolve $^{12}C^{+}$ from $^{24}Mg^{2+}$, $^{32}S^{+}$ from $^{16}O_2^{+}$ etc.

In-situ major element analyses were obtained by EPMA using a JEOL JXA 8230 system at Victoria University of Wellington (VUW), or using a CAMECA SX100 at the University of Edinburgh, both using wavelength-dispersive spectrometry. Precision of standard analyses of major elements (>5 wt.% concentration) is always within 2 relative % (2 s.d.); uncertainties are slightly higher for minor elements. Due to their hydrated nature only glass analyses with totals of <93 wt.% were set aside; values for the remaining analyses were then normalised to 100 %. Prior to analysis, back-scattered electron (BSE) images were taken of all melt inclusions and crystal phases to identify zoning patterns and locate analytical spots. This was carried out VUW using the EPMA, and at UEA using a JEOL JSM 5900LV scanning electron microscope (SEM).

Trace element analyses of crystal phases and matrix glass were carried out at the University of Durham using New Wave deep UV laser (193 nm solid state) coupled to an X-series 2 ICPMS. Analyses were run using a 35 μm spot. The LA-ICPMS data were internally normalized to ^{29}Si or ^{43}Ca from EPMA analyses. Abundances of single trace elements were calculated relative to a bracketing standard (NIST 612) which was analysed throughout the run under identical conditions. Precision and accuracies varied depending on the analytical conditions but generally have <10% (2 s.d.) uncertainties (see Electronic Appendix).

RESULTS

Whole rock major and trace elements

XRF analyses of samples taken at seven intervals through the fall deposit (for sampling interval details see Table 1; full results in electronic appendix) were analysed to complement the detailed crystal and glass analyses from the three identified subunits (see below). Systematic changes in most major and trace elements analysed are evident, with the upper-most sample of trachy-basaltic andesite (i.e. the top of subunit C) being enriched in MgO, Fe_2O_3, CaO, TiO_2, P_2O_5, V and Sr relative to all stratigraphically-lower samples (Fig. 5). In contrast, the lower-most trachytic sample is enriched in SiO_2, K_2O, Na_2O, Rb, Zr, Nb, Ba, La, Ce (Fig. 5) relative to all stratigraphically-higher samples, while there is no measureable change in MnO, Al_2O_3, Ni, Cu, Cr, ZN, Y, Pb, Th or U throughout the deposit.

Petrography

The ~~compositionally~~ zoned fall is a crystal-poor deposit, with less than 5% crystals (by volume). The dominant crystal phases (in decreasing order of abundance) are plagioclase feldspar + olivine ± anorthoclase feldspar + ilmenite + magnetite~~.~~, and all are < 0.5mm in diameter. Rare accessory phases of apatite and allanite are occasionally present. Clinopyroxene is present only in the upper, more mafic compositions. BSE images of the two feldspars, olivine, clinopyroxene and Fe–Ti oxides show no visible zoning, and all crystal phases are euhedral (Fig. 6). ~~Crystal phases are always unzoned in back-scattered electron (BSE) imagery (Fig. 6), and~~ Olivine is typically melt inclusion –rich, with multiple melt inclusions per crystal and ~~and~~ melt ~~inclusions~~inclusions are occasionally linked to the exterior of the crystal, giving an embayed appearance (Fig. 6a, b). However, there is no evidence ~~all crystal phases are euhedral with no evidence~~in any other crystal phases ~~for~~ any dissolution having occurred. ~~Olivine is typically melt inclusion-rich, with multiple melt inclusions per crystal.~~

Phenocryst compositions

Major and trace element analyses of feldspars were carried out on samples from the three subunits of the ~~compositionally~~ zoned fall. Two populations of feldspars are identified (Fig. 7a) - a sanidine-anorthoclase component ($An_2Or_{38}Ab_{60}$), and an andesine component ($An_{40}Or_2Ab_{58}$). There is no systematic difference between core and rim analyses in any subunit sample, and neither feldspar populations have any observable zonation visible in BSE imagery (Fig. 6). Similarly, crystal habits are euhedral, with no textural evidence for textural disequilibrium between the melt and the two feldspar groups. Feldspars from the three subunits are overlapping in their feldspar compositions with no major variations apparent, however feldspars from subunits B and C have slightly higher Sr concentrations at lower silica concentrations than feldspars from subunit A (Fig. 7a).

Major and trace element analyses of olivine crystals show a range in compositions from Fo_{45} to Fo_8 (Fig. 7b). Similar to the feldspar, the olivine shows no systematic variation between cores and rims, or within subgroups. While all three subunits have overlapping olivine compositions, subunits B and C extend to slightly higher forsterite compositions at lower MnO concentrations (Fig. 7b).

Matrix glass and melt inclusions

Major and trace element analyses of melt inclusions and matrix glass are overlapping, and span a range of ~55 wt.% SiO_2 to ~70 wt.% SiO_2 (Fig. 8). Glass analyses of major and trace elements show a systematic difference between subunits, with subunit A being the most-evolved (SiO_2 63 – 70 wt.%), subunit B being transitional (SiO_2 59 – 66 wt.%), and subunit C having the least-evolved glass compositions (SiO_2 55 – 63 wt.%; Fig. 8a). Subunit A is also enriched in K_2O, Na_2O, Rb, Zr, Ba, the light rare earth elements (LREE) and Pb, whilst being depleted in TiO_2, FeO, MgO, CaO, P_2O_5, Sr and Eu relative to subunit C (see Fig. 8 and Electronic Appendix).

SEM images of melt inclusions reveal many ~~inclusions which~~inclusions that are not fully entrapped (Fig. 6), with the potential that some inclusions whilst appearing isolated in 2 dimensions may be connected to an exterior surface in three dimensions. While care was taken to analyse only fully enclosed inclusions, some results show clear influence of post-entrapment degassing (Fig. 8). Volatile concentrations measured in the melt inclusions are variably degassed, and therefore do not reflect primary volatile concentrations (Fig. 8c, d). However, un-degassed melt inclusions from all subunits show H_2O concentrations between 2 and 4 wt.%, and show a weak negative correlation with key trace elements sensitive to fractional crystallisation such as Sr and Eu (Fig. 8c, d). CO_2 concentrations are ~~between (200 and 1000 – 100~~ up to 1000 ppm (Fig. 8c). Concentrations of halogens in un-degassed melt inclusions do not show any discernible differences between the identified subunits, and do not correlate with any measured trace element (see Electronic Appendix).

MAGMATIC CONDITIONS

Temperature & fO_2

EPMA analyses of coexisting Fe–Ti oxides were undertaken, and tested for equilibrium using the calculations of Bacon & Hirschman (1988). All pairs that were within the allowable bounds were then used to model equilibrium temperatures and oxygen fugacities of the coexisting Fe–Ti oxides, using the calibrations of Ghiorso & Evans (2008). Results are displayed in Table 2. Oxides from subunit A yield an ~~modelled~~ average model temperature of 845 °C with an oxygen fugacity of -2.28 log units relative to the Nickel- Nickel Oxide (NNO) buffer. In subunit C, average modelled temperatures are 866 °C, and fO_2 of -1.94 log units ΔNNO. Given the commonly cited uncertainties of ± 30 °C associated with Fe–Ti oxide thermometry (e.g. Blundy & Cashman, 2008) these results indicate limited resolvable differences in temperature between the samples of the zoned fall. Hence, there is little

evidence for a thermal gradient existing within the magmatic system in the months to weeks prior to eruption.

The highly reducing fO_2 of the system is surprising given the high H_2O concentrations measured in melt inclusions (Fig. 8; Electronic Appendix), given that it is normally inferred that the fO_2 and H_2O systematics are coupled (Lee et al., 2005). However, the calculated oxygen fugacities are in line with the observed mineralogy (fayalite-rich) and the tectonic (ocean island) setting (~~being an ocean island;~~ Carmichael, 1991). It is not thought that fO_2 is affected by fractionation processes, and therefore can maintain the relatively reduced nature of the magma, whilst H_2O proportions are systematically increasing due to its generally incompatible behaviour in the fractionating phases (Carmichael, 1991; Portnyagin et al., 2012). Thus, we see evidence for decoupling of the H_2O and fO_2 systematic at Ascension Island, similar to that suggested at Hekla volcano, Iceland (Portnyagin et al., 2012).

Pressure

Entrapment pressures for the measured melt inclusions were calculated using the MagmaSat application developed from Gualda & Ghiorso (2014) which takes into account not only the measured volatile concentrations, but also the major element composition of the host melt inclusion. A single temperature of 850 °C, based on our Fe–Ti oxide thermometry, was used to calculate entrapment pressures. Given the potentially 'leaky' morphology of our olivine-hosted melt inclusions (Fig. 6) in 3D, the maximum entrapment pressures for each unit were taken as the true entrapment pressures (Table 2), but the range in modelled pressures clearly shows the effect of some partial degassing of the inclusions during ascent of the magmas (Fig. 9). There is no systematic difference in entrapment pressures between all three subunits of the ~~compositionally~~ zoned fall. These entrapment pressures of ~2540 MPa correspond to a depth of ~8.5 km (assuming a crustal density of 3000 kg/m^3); the base of the oceanic crust at Ascension (Klingelhöfer et al., 2001). It is important to note that these modelled entrapment pressures only represent the pressure at which crystal were growing and trapping melt inclusions, and there is no record preserved of any magmatic evolution (and the depths at which that occurred) prior to crystal growth.

DISCUSSION

The gradationally zoned fall deposit, zoned in composition but not temperature, is a unique deposit on Ascension Island. Here we discuss the nature of the stratification, causes for the

stratification within the magma chamber, eruption triggering mechanisms and how representative these processes are for all evolved magmatism on Ascension Island.

Evolution of the zoned fall

~~Evolutionary processes within the melt dominant magma body prior to eruption can be tracked by looking at both melt inclusions and matrix glass.~~ The modelled entrapment pressures from melt inclusions within crystal cores compared with those trapped in crystal rims, are overlapping. We thus consider that the crystals grew within a stalled body of magma, rather than representing crystal growth and melt inclusion entrapment upon ascent. Thus, we use melt inclusion and matrix glass compositions to look at the evolutionary processes occurring within the melt dominant magma body prior to eruption. We first consider the nature of the final stratification of the zoned fall magma body:

Final stratification

There are two potential causes for the gradational stratification preserved in the whole rock and matrix glass chemistry (Figs. 5, 8a); either two compositionally distinct magmas interacted, mixed and homogenised (i.e. in an open-system); or a single magma batch stalled and evolved (i.e. in a closed-system). If the first case occurred~~is occurring~~ we would expect to see bimodality in both phenocryst and trapped melt inclusion~~s~~ compositions, potentially with some evidence for disequilibrium textures within the crystal cargo. However, as previously shown, all crystals appear to be in equilibrium with the melt in which they were erupted (Fig. 6): there is no evidence for chemical changes recorded within crystal interiors (cf. Morgan et al., 2004; Sliwinski et al., 2015). Furthermore while melt inclusion entrapment pressures could represent re-homogenization of melt inclusions at a stalling point, this appears unlikely given that~~Similarly,~~ melt inclusion compositions are very similar to those of matrix glasses (Fig. 8a). The overlap in entrapment pressures from all units, lack of zonation within crystals, and overlapping melt inclusion and matrix glass compositions shows that~~and therefore we see no evidence for any~~ no magma mixing, prior to crystal growth in the melt dominant body, has occurred, ~~-~~and yet the chemical zonation remains. Therefore the compositional zonation sampled by the zoned fall deposit on Ascension Island appears to have been generated by closed-system evolution in a single magma chamber.

Role of fractional crystallisation

In order to assess the role of fractional crystallisation in generating the zoned fall deposit, we applied the least-squares modelling technique of Stormer and Nichols (1978) though the

PetroGraph model of Petrelli et al. (2005) to the major element compositions. Whole rock compositions of subunit C (i.e. the least-evolved; Fig. 5) are used as our starting compositions. Fractionating phase compositions are modelled from our EPMA analyses of crystal phases present in subunit C (see Electronic Appendix)~~,~~. H~~h~~owever, apatite (which is present as a minor component in many Ascension Island rocks, Kar et al., 1998) was not directly measured, so an average composition was taken from Stock et al. (2016). The results of this fractionation modelling (where the sum of the residuals is < 0.12) reveals that the least-evolved magma composition can be directly related to the magma composition of subunit A (i.e. the most-evolved; Fig. 5) by simple crystal fractionation, dominated by plagioclase feldspar (61.6%) and olivine (22.5%) (mirroring the dominant crystal phases, see results). Fractionation of minor amounts of Fe~~–~~-Ti oxides (6.3%), clinopyroxene (5.7%) and apatite (3.9%) also contribute to the evolution of least- to most-evolved magma compositions in the zoned fall deposit. Interestingly, this modelling also suggests that the unzoned sanidine-anorthoclase feldspar (see results) is an accumulated, rather than fractionated phase, although the role this plays in developing the zonation within the zoned fall is minor. These more-evolved anorthoclase feldspars are likely to be sourced from surrounding plutonic bodies (studied by Harris, 1983; Kar et al., 1998; Webster & Rebbert, 2001) which are present in the surrounding crust, and often appear as lithic clasts within many fall deposits on Ascension Island (Hobson, 2001).

The lack of significant open-system behaviour in the generation of the zoned fall deposit on Ascension Island contrasts with many other ocean island volcanoes such as Iceland and Tenerife, where there is significant evidence for magma mixing and crustal assimilation (e.g. Ablay et al., 1998; Sverisdottir, 2007; Carley et al., 2011; Kuritani et al., 2011; Wiesmaier et al., 2013). Currently, there is no geothermal activity present on Ascension Island, with heat flow measurements ranging from 75 to 124 mW/m^2 (Nielson et al., 1996) in shallow (< 600 m) boreholes drilled on the island. This is much lower than other ocean islands where geothermal power plants exploit the high heat flows from magmatism (e.g. Iceland) but whether this is representative of the entirety of Ascension's volcanic history, or if reflects a potential cessation of volcanism at Ascension is not known. However, given the relatively slow volcanic growth rates modelled by Minshull et al. (2010) of 0.4 km/Myr (compared with average growth rates of 4.6 km/Myr of Mauna Kea during both its shield building stage, and post-shield stage; Sharp & Renne, 2005), it would seem that rates of magma flux during Ascension's volcanic history have been low, and thus favour closed-system evolution with limited magma mixing.

Convection in a stratified magma body?

The detailed field data show that the zoned fall deposit was erupted from a single vent source. Further to this, the geochemical analyses, reveal a systematic gradation (e.g. Figs. 5 – 8), and therefore confirm that the deposit is the result of the evacuation of a single zoned magma body. In order for this compositional stratification to be preserved so well on a deposit scale, the magma chamber must not have experienced significant syn-eruptive mixing, and equally convection within the magma chamber must have had relatively little influence on the stratification, once crystals were forming, in order to preserve the zoning within the magma chamber.

It seems likely that no chamber-wide convection was occurring due to reasons discussed above, however this raises questions as to why convection was not occurring. We see no evidence for a thermal stratification in the magma body, with no systematic differences in modelled Fe–Ti oxide temperatures from the upper and lower regions of the magma body. This does not negate the effect of crystallisation on the walls of the magma chamber driving any convection, yet the relatively deep location of the storage region (~ 8.5 km, see above) compared to the depth to the Moho (~12 km; Klingelhöefer et al., 2001) and the higher geothermal gradient in oceanic lithosphere may mean that this effect is minimal when compared with magma storage zones on continents. However, given the lack of evidence for new magmatic influx into the storage region, there will be a finite time period over which the stored magma remains in an eruptible state. Lack of convective heat loss and latent heat of crystallisation will maintain eruptive temperature (e.g. Karlstrom et al., 2009) and counteract the conductive heat loss to the surrounding lithosphere. Estimation of the maximum timescales for residence would require better knowledge of the chamber volume and geometry than is provided by the erupted deposits. However, we would suggest that the eruptive window (the timescale over which a magma remains in an 'eruptible state') must be comparatively short, in the absence of any influx of new, hotter material. Available field evidence (rapid attenuation in deposit thickness over distances) would suggest that the erupted volume was comparatively small.

Eruptive triggers

Understanding the triggering mechanisms of volcanic eruptions is vital for monitoring active volcanoes and forecasting future activity. Commonly cited triggers range from internal triggers due to overpressure from volatile oversaturation or magmatic intrusion (e.g. Jellinek

& DePaolo, 2003; Caricchi et al., 2014) or magma mixing driving catastrophic destabilisation of the magmatic system (e.g. Saunders et al., 2012; Albino and Sigmundsson, 2014; Till et al., 2015). External triggers, outside of the magmatic system include tectonic activity (e.g. Allan et al., 2012) or changing stress-state (e.g. Bonali et al., 2013).

~~Ascension Island's location within 100 km of the MAR, and within 50 km of the AFZ, means that there will be earthquakes > magnitude 4 in the region, which could affect magma chamber stability (Manga and Brodsky et al., 2006). However, there is no direct evidence to link the eruption of the zoned fall to any regional tectonic activity; with all phases being in apparent equilibrium with their surrounding melt. Magmatic evolution appears to have proceeded in a relatively stable tectonic environment (see Evolution of zoned fall section above).~~

One of the more commonly citerd eruptive triggers is magma maixing, yet ~~Similarly,~~ there is no evidence for magma mixing preserved in the pumice or scoria clasts of the zoned fall deposit and magma evolution appears to have occurred in a closed-system with no subsequent perturbation of the system (Fig. 6 – 8). The apparently low magmatic flux, when compared with other ocean islands such as Iceland, Hawaii and the Canary Islands, ~~appears to~~may have allowed~~to allow~~ the magma responsible for the zoned fall to ~~not have interacted~~ remain isolated ~~with any other~~from other magmatic~~magma composition~~ pulses (cf. Sverisdottir, 2007; Albert et al., 2016). Therefore magma mixing was not an eruptive trigger for the eruption of the zoned fall.

Another potential eruptive trigger is tectonic activity. Ascension Island's location within 100 km of the MAR, and within 50 km of the AFZ, means that there will be earthquakes of magnitudes greater than 4 in the region, which could affect magma chamber stability (Manga and Brodsky et al., 2006). No direct evidence is preserved in the crystal or melt compositions to link the eruption of the zoned fall to any regional tectonic activity; with all phases being in apparent equilibrium with their surrounding melt. Magmatic evolution appears to have proceeded in a relatively stable tectonic environment (see Evolution of zoned fall section above). Yet, we cannot preclude earthquake activity as an eruptive trigger, that left no record in the crystal cargo (cf. Allan et al., 2012).

Internal overpressure within a closed system is another potential eruptive trigger, where crystal fractionation increases the concentration of magmatic volatiles in the magma (cf. Tait et al., 1989). The high H_2O contents measured in melt inclusions (up to 4 wt%), and well-understood role of closed-system evolution of the zoned fall make this the most plausible eruptive trigger, as H_2O has the greatest effect in generating overpressures in

Formatted: Indent: First line: 1.27 cm

magma, due to its more soluble nature (Tait et al., 1989, Stock et al., 2016). ~~Therefore, we suggest that~~Therefore, the eruption of the zoned fall ~~of the zoned fall deposit on Ascension Island~~ appears to have been~~was~~ primed ~~triggered~~ by increasing internal overpressurisatione due to volatile oversaturation. ~~due to fractionation increasing the concentration of magmatic volatiles in the magma (cf. Tait et al., 1989). The high H_2O contents measured in melt inclusions (up to 4 wt.%) make this even more likely, as H_2O has the greatest effect in generating overpressures in magma, due to its more soluble nature (Tait et al., 1989).~~ However, while volatile oversaturation undoubtedly primed the magma body for eruption, the trigger may have been a combination of factors, including local earthquake activity, of which no record is preserved.

Generation of silicic magmas at Ascension Island

The zoned fall deposit is only one of multiple felsic explosive deposits on Ascension Island, in its ~ 1 Myr subaerial history (Kar et al., 1998; Hobson, 2001; Jicha et al., 2014). Previous work has investigated the origins of evolved magmas on Ascension Island (Kar et al., 1998), and there has been only minor petrological investigation of eruptions (generally only the evolved lavas: Harris 1983) and none has benefitted from a well-established volcanic stratigraphy, or precise eruption dates, to be able to test if magmatic processes and timescales vary with time on Ascension Island. Previous work has suggested varying importance for the roles of both fractional crystallisation and assimilation (see Kar et al., 1998; Weaver et al., 1998; Webster & Rebbert, 2001), with some older work even suggesting the presence of a single large magma chamber feeding Ascension Island silicic volcanism (Kar et al., 1998). In this instance, it is clear that fractional crystallisation and minor amounts of crystal accumulation in a relatively closed magmatic system is responsible for the generation of the compositional zonation preserved in the studied fall deposit. It is interesting to note that the difference between most- and least-evolved compositions sampled by the zoned fall deposit is not large (54.5 wt.% SiO_2 at the top of the deposit to 60.5 wt.% SiO_2 at the deposit base; Fig. 5 and Electronic Appendix)- it is possible that all pumice fall deposits on Ascension Island are compositionally zoned, but did not cross the pumice-scoria textural boundary, and thus appear unzoned in the field. Further work is required to test for zonation in any of the other explosive silicic deposits.

The generally closed-system evolution of the zoned fall makes Ascension Island appear anomalous when compared with other classic ocean island volcanoes such as Hawaii, Iceland and the Canaries (see above). Similarly, the zoned fall appears anomalous in that

there is only evidence for a single stage of evolution in both the melt inclusions and crystal cargos examined. This contrasts with many other ocean islands that preserve evidence for polybaric fractionation (for example Tenerife: Sliwinski et al., 2015; Iceland: Mancini et al., 2015; the Azores: Genske et al., 2012). It seems unlikely that the less-evolved end-member of the zoned fall deposit is a parental magma for Ascension, due to its generally more-evolved composition than many other Ascension lavas (see grey shaded area on Fig. 5a). Therefore this magma must have differentiated prior to evolution within the zoned fall magma reservoir. That this stage is not preserved in any crystals present in the zoned fall implies effective liquid-crystal separation at an earlier stage of evolution, potentially feasible due to the lower viscosity of the alkaline magmas at Ascension.

CONCLUSIONS

By studying the zoned fall deposit on Ascension Island we have garnered significant insights into the generation of this deposit, but have also raised questions regarding the generation and evolution of silicic magmas at Ascension Island and other ocean island volcanoes. Our main conclusions are summarised below:

1. A unique zoned fall deposit on Ascension Island displays a systematic gradation in composition, grading from trachyte at the base, to trachy-basaltic andesite at the top of the deposit. This zonation results from the evacuation of a single compositionally (but not thermally) zoned magma batch residing at ~8.5 km depth: the base of oceanic crust at Ascension.
2. The zonation within the magma body occurred through closed-system crystal fractionation of mainly feldspar and olivine, with minor amounts of clinopyroxene, Fe–Ti -oxides and apatite, and the accumulation of a sanidine-anorthoclase feldspar phase, likely to be from older plutonic bodies present in the crust. This relatively simple evolutionary path for the generation of evolved magmas in thin oceanic lithosphere at Ascension contrasts with many other ocean island volcanoes, where magma supply rates are higher and therefore favour more complex magmatic interactions and open system behaviour.
3. The eruption of the zoned fall deposit appears to have been ~~was~~ internally triggered, via fractional crystallisation concentrating volatiles into the melt phase, and eventually leading to over-pressurisation. This is supported by the high volatile content melt inclusions; the lack of any hydrous crystal phases that could accommodate increased H_2O concentrations; and the lack of evidence for magma mixing. While there~~There~~ is

no geochemical evidence for tectonics triggering the eruption of the zoned fall deposit (cf. Allan et al., 2012), this may not be recorded in the crystal cargo, and thus a tectonic role in the eruption of the zoned fall cannot be precluded.~~.~~

4. The data show a lack of apparent coupling between reducing oxygen fugacities in the zoned fall on Ascension Island (fO_2 ~ -2.2 log units ΔNNO) and elevated H_2O contents (up to 4 wt.% H_2O) similar to that observed by Portnyagin et al. (2012) in Iceland. Thus, while the source of Ascension Island magmas may be reducing (and therefore impart a reduced oxygen fugacity on the magma) this is not affected by evolution and fractionation. Yet, due to the absence of hydrous crystal phases on Ascension Island, H_2O contents increase in the magma body with increasing degrees of evolution, yielding water-rich erupted magma compositions.
5. The zonation preserved in the zoned fall deposit on Ascension, highlighted by the textural change from pumice at the base to scoria at the top of the deposit, may be present in other fall deposits on Ascension, whose composition does not cross the pumice-scoria textural boundary. Further work is needed to assess how applicable the magmatic processes responsible outlined here are to all silicic volcanism on Ascension Island.

ACKNOWLEDGEMENTS

The Ascension Island Government , and Administrator Marc Holland, the Ascension Island Heritage Society, Conservation Department and Ascension Island residents, in particular Drew Avery and Holly Connolly, are thanked for their logistical support during field seasons. Richard Hinton, John Craven and Cees-Jan de Hoog at the Edinburgh Ion Microprobe Facility are thanked for their support during our analytical session there. We are grateful to Chris Hayward, Ian Schipper, Bertrand Lezé, Chris Ottley and George Cooper for their laboratory and technical assistance during the course of analyses for this project. The authors wish to thank Margaret Mangan, Brian Jicha and an anonymous reviewer for their prompt and constructive reviews and the efficient handling of this submission. This project was funded by a Leverhulme Trust Research Project Grant (RPG-2013-042), with the second field season supported by a Gloyne Outdoor Geological Research award from the Geological Society of London. Ion microprobe time was funded by the Natural Environment Research Council.

REFERENCES

Ablay, G. J., Carroll, M. R., Palmer, M. R., Martí, J., & Sparks, R. S. J. (1998). Basanite–phonolite lineages of the Teide–Pico Viejo volcanic complex, Tenerife, Canary Islands. *Journal of Petrology*, *39*(5), 905-936.

Albert, H., Costa, F., & Martí, J. (2016). Years to weeks of seismic unrest and magmatic intrusions precede monogenetic eruptions. *Geology*, *44*(3), 211-214.

Albino, F., & Sigmundsson, F. (2014). Stress transfer between magma bodies: Influence of intrusions prior to 2010 eruptions at Eyjafjallajökull volcano, Iceland. *Journal of Geophysical Research: Solid Earth*, *119*(4), 2964-2975.

Allan, A. S., Wilson, C. J., Millet, M. A., & Wysoczanski, R. J. (2012). The invisible hand: tectonic triggering and modulation of a rhyolitic supereruption. *Geology*, *40*(6), 563-566.

Bacon, C. R. & Hirschmann, M. M. (1988). Mg/Mn partitioning as a test for equilibrium between coexisting Fe^Ti oxides. *American Mineralogist 73*, 57-61

Blundy, J., & Cashman, K. (2008). Petrologic reconstruction of magmatic system variables and processes. *Reviews in Mineralogy and Geochemistry*, *69*(1), 179-239.

Bonadonna, C., Cioni, R., Pistolesi, M., Connor, C., Scollo, S., Pioli, L., & Rosi, M. (2013). Determination of the largest clast sizes of tephra deposits for the characterization of explosive eruptions: a study of the IAVCEI commission on tephra hazard modelling. *Bulletin of volcanology*, *75*(1), 1-15.

Bonali, F. L., Tibaldi, A., Corazzato, C., Tormey, D. R., & Lara, L. E. (2013). Quantifying the effect of large earthquakes in promoting eruptions due to stress changes on magma pathway: the Chile case. *Tectonophysics*, *583*, 54-67.

Caricchi, L., Annen, C., Blundy, J., Simpson, G. & Pinel, V. (2014). Frequency and magnitude of volcanic eruptions controlled by magma injection and buoyancy. *Nature Geoscience 7*, 126–130.

Carley, T. L., Miller, C. F., Wooden, J. L., Bindeman, I. N., & Barth, A. P. (2011). Zircon from historic eruptions in Iceland: reconstructing storage and evolution of silicic magmas. *Mineralogy and Petrology*, *102*(1-4), 135-161.

Carmichael, I. S. (1991). The redox states of basic and silicic magmas: a reflection of their source regions? *Contributions to Mineralogy and Petrology*, *106*(2), 129-141.

Daly, R. A. (1925, June). The geology of Ascension island. In *Proceedings of the American Academy of Arts and Sciences* (Vol. 60, No. 1, pp. 3-80). American Academy of Arts & Sciences.

Gazel, E., Hayes, J. L., Kelemen, P. B., Everson, E. D., Holbrook, W. S., & Vance, E. (2014, December). Generation of continental crust in intra-oceanic arcs. In *AGU Fall Meeting Abstracts* (Vol. 1, p. 4845).

Genske, F. S., Turner, S. P., Beier, C., & Schaefer, B. F. (2012). The petrology and geochemistry of lavas from the western Azores islands of Flores and Corvo. *Journal of Petrology*, *53*(8), 1673-1708.

Ghiorso, M. S., & Evans, B. W. (2008). Thermodynamics of rhombohedral oxide solid solutions and a revision of the Fe-Ti two-oxide geothermometer and oxygen-barometer. *American Journal of Science*, *308*(9), 957-1039.

Gualda, G. A., & Ghiorso, M. S. (2014). Phase-equilibrium geobarometers for silicic rocks based on rhyolite-MELTS. Part 1: Principles, procedures, and evaluation of the method. *Contributions to Mineralogy and Petrology*, *168*(1), 1-17.

Harris, C. (1983). The petrology of lavas and associated plutonic inclusions of Ascension Island. *Journal of Petrology*, *24*(4), 424-470.

Hobson, K.E. (2001). The pyroclastic deposits and eruption history of Ascension Island: a palaeomagnetic and volcanological study. *Doctoral dissertation, University of Oxford*.

Humphreys, M., Kearns, S.L. and Blundy, J.D., 2006. SIMS investigation of electron-beam damage to hydrous, rhyolitic glasses: Implications for melt inclusion analysis. *American Mineralogist*, *91*(4), 667-679.

Jellinek, A. M., & DePaolo, D. J. (2003). A model for the origin of large silicic magma chambers: precursors of caldera-forming eruptions. *Bulletin of Volcanology*, *65*(5), 363-381.

Jicha, B. R., Singer, B. S., & Valentine, M. J. (2013). 40Ar/39Ar Geochronology of Subaerial Ascension Island and a Re-evaluation of the Temporal Progression of Basaltic to Rhyolitic Volcanism. *Journal of Petrology*, *54*(12), 2581-2596.

Kar, A., Weaver, B., Davidson, J., & Colucci, M. (1998). Origin of differentiated volcanic and plutonic rocks from Ascension Island, South Atlantic Ocean. *Journal of Petrology*, *39*(5), 1009-1024.

Karlstrom, L., Dufek, J., & Manga, M. (2009). Organization of volcanic plumbing through magmatic lensing by magma chambers and volcanic loads. *Journal of Geophysical Research: Solid Earth*, *114*(B10).

Klingelhöfer, F., Minshull, T. A., Blackman, D. K., Harben, P., & Childers, V. (2001). Crustal structure of Ascension Island from wide-angle seismic data: implications for the formation of near-ridge volcanic islands. *Earth and Planetary Science Letters*, *190*(1), 41-56.

Kuritani, T., Yokoyama, T., Kitagawa, H., Kobayashi, K., & Nakamura, E. (2011). Geochemical evolution of historical lavas from Askja Volcano, Iceland: Implications for mechanisms and timescales of magmatic differentiation. *Geochimica et Cosmochimica Acta*, *75*(2), 570-587.

Lee, C. T. A., Leeman, W. P., Canil, D., & Li, Z. X. A. (2005). Similar V/Sc systematics in MORB and arc basalts: implications for the oxygen fugacities of their mantle source regions. *Journal of Petrology*, *46*(11), 2313-2336.

Malfait, W.J., Seifert, R., Petitgirard, S., Perrillat, J.P., Mezouar, M., Ota, T., Nakamura, E., Lerch, P. and Sanchez-Valle, C., 2014. Supervolcano eruptions driven by melt buoyancy in large silicic magma chambers. *Nature Geoscience*, *7*(2), 122-125.

Mancini, A., Mattsson, H. B., & Bachmann, O. (2015). Origin of the compositional diversity in the basalt-to-dacite series erupted along the Heiðarsporður ridge, NE Iceland. *Journal of Volcanology and Geothermal Research*, *301*, 116-127.

Manga, M. and Brodsky, E., 2006. Seismic triggering of eruptions in the far field: volcanoes and geysers. *Annu. Rev. Earth Planet. Sci*, *34*, 263-291.

Minshull, T. A., Ishizuka, O., & Garcia‐Castellanos, D. (2010). Long‐term growth and subsidence of Ascension Island: Constraints on the rheology of young oceanic lithosphere. *Geophysical Research Letters*, *37*(23).

Morgan, D. J., Blake, S., Rogers, N. W., DeVivo, B., Rolandi, G., Macdonald, R., & Hawkesworth, C. J. (2004). Time scales of crystal residence and magma chamber volume from modelling of diffusion profiles in phenocrysts: Vesuvius 1944. *Earth and Planetary Science Letters*, *222*(3), 933-946.

Mortensen, A. K., Wilson, J. R., & Holm, P. M. (2009). The Cão Grande phonolitic fall deposit on Santo Antão, Cape Verde Islands. *Journal of Volcanology and Geothermal Research*, *179*(1), 120-132.

Nielson, D. L., & Sibbett, B. S. (1996). Geology of Ascension Island, South Atlantic Ocean. *Geothermics*, *25*(4), 427-448.

Nielson, D. L., Adams, M. C., Sibbett, B. S., & Wright, P. M. (1996). Shallow thermal structure and hydrology of Ascension Island, south Atlantic Ocean. *Geothermics*, *25*(4), 521-541.

Pallister, J. S., Hoblitt, R. P., & Reyes, A. G. (1992). A basalt trigger for the 1991 eruptions of Pinatubo Volcano? *Nature*, 356, 426-428.

Petrelli, M., Poli, G., Perugini, D., & Peccerillo, A. (2005). PetroGraph: A new software to visualize, model, and present geochemical data in igneous petrology. *Geochemistry, Geophysics, Geosystems*, *6*(7).

Portnyagin, M., Hoernle, K., Storm, S., Mironov, N., van den Bogaard, C., & Botcharnikov, R. (2012). H 2 O-rich melt inclusions in fayalitic olivine from Hekla volcano: implications for phase relationships in silicic systems and driving forces of explosive volcanism on Iceland. *Earth and Planetary Science Letters*, *357*, 337-346.

Saunders, K., Blundy, J., Dohmen, R., & Cashman, K. (2012). Linking petrology and seismology at an active volcano. *Science*, *336*(6084), 1023-1027.

Sharp, W. D., & Renne, P. R. (2005). The 40Ar/39Ar dating of core recovered by the Hawaii Scientific Drilling Project (phase 2), Hilo, Hawaii. *Geochemistry, Geophysics, Geosystems*, *6*(4).

Sliwinski, J. T., Bachmann, O., Ellis, B. S., Dávila-Harris, P., Nelson, B. K., & Dufek, J. (2015). Eruption of Shallow Crystal Cumulates during Explosive Phonolitic Eruptions on Tenerife, Canary Islands. *Journal of Petrology*, egv068.

Snyder, D., 2000. Thermal effects of the intrusion of basaltic magma into a more silicic magma chamber and implications for eruption triggering. *Earth and Planetary Science Letters*, *175*(3), 257-273.

Snyder, D. C., Widom, E., Pietruszka, A. J., Carlson, R. W., & Schmincke, H. U. (2007). Time scales of formation of zoned magma chambers: U-series disequilibria in the Fogo A and 1563 AD trachyte deposits, São Miguel, Azores. *Chemical geology*, *239*(1), 138-155.

Sparks, S.R. & Sigurdsson, H., 1977. Magma mixing: a mechanism for triggering acid explosive eruptions. *Nature*, *267*, 315-318.

Stock, M.J., Humphreys, M.C., Smith, V.C., Isaia, R. and Pyle, D.M., 2016. Late-stage volatile saturation as a potential trigger for explosive volcanic eruptions. *Nature Geoscience*, *9*(3), 249-254.

Stormer, J. C., & Nicholls, J. (1978). XLFRAC: a program for the interactive testing of magmatic differentiation models. *Computers & Geosciences*, *4*(2), 143-159.

Sverrisdottir, G. (2007). Hybrid magma generation preceding Plinian silicic eruptions at Hekla, Iceland: evidence from mineralogy and chemistry of two zoned deposits. *Geological Magazine*, *144*(04), 643-659.

Tait, S., Jaupart, C., & Vergniolle, S. (1989). Pressure, gas content and eruption periodicity of a shallow, crystallising magma chamber. *Earth and Planetary Science Letters*, *92*(1), 107-123.

Till, C. B., Vazquez, J. A., & Boyce, J. W. (2015). Months between rejuvenation and volcanic eruption at Yellowstone caldera, Wyoming. *Geology*, *43*(8), 695-698.

Walker, G. P. (1966). Acid volcanic rocks in Iceland. *Bulletin Volcanologique*, *29*(1), 375-402.

Watanabe, S., Widom, E., Ui, T., Miyaji, N., & Roberts, A. M. (2006). The evolution of a chemically zoned magma chamber: The 1707 eruption of Fuji volcano, Japan. *Journal of volcanology and geothermal research*, *152*(1), 1-19.

Weaver, B., Kar, A., Davidson, J., & Colucci, M. (1996). Geochemical characteristics of volcanic rocks from Ascension Island, south Atlantic Ocean. *Geothermics*, *25*(4), 449-470.

Webster, J. D., & Rebbert, C. R. (2001). The geochemical signature of fluid-saturated magma determined from silicate melt inclusions in Ascension Island granite xenoliths. *Geochimica et Cosmochimica Acta*, *65*(1), 123-136.

Wiesmaier, S., Troll, V. R., Wolff, J. A., & Carracedo, J. C. (2013). Open-system processes in the differentiation of mafic magma in the Teide–Pico Viejo succession, Tenerife. *Journal of the Geological Society*, *170*(3), 557-570.

FIGURE CAPTIONS

Figure 1: Ascension Island location map (a) shown in relation to the Mid Atlantic Ridge, the Ascension Fracture Zone (AFZ) and the Bode Verde Fracture Zone (BVFZ). Geological map of Ascension Island (b) showing the areas where lavas, scoria cones and pyroclastic deposits are exposed at the surface. Faults are shown as red lines.

Figure 2: Zoned fall deposit of Ascension Island. (a) The compositionally zoned fall at showing the three transitional subunits A to C, and the overlying scoria. Notebook is 205 mm wide for scale. Representative stratigraphic log through the zoned fall along with subunit descriptions (b). Lithic clasts are shown as black~~rown~~ clasts, with pumice as white clasts and scoria as brown~~dark grey~~ clasts. Colour of juvenile clasts relates only to their textural association, rather than retaining any compositional information, or reflecting the colours of the juvenile clasts in the subunits. Clasts shown to scale.

Figure 3: Zoned fall localities (pink stars) overlain over the geological map of Ascension (area shown in Fig. 1). The numbers for the ~~compositionally~~ zoned fall outcrops indicate total unit thickness in cm, the geometric mean of the 5 largest pumice dimension in subunit A, in mm (following Bonadonna et al., 2013) and the geometric mean of the 5 largest lithic clasts in A, in mm (following Bonadonna et al., 2013). Where no thickness is given, the full sequence of the unit has not been preserved. Locations where samples were collected are outlined in yellow, with the unit outlined in yellow and green being the location where all samples of subunits A, B and C analysed for melt inclusions were collected.

Figure 4: Juvenile clasts from the 3 subunits of the ~~compositionally~~ zoned fall deposit from pumice in subunit A, through to scoria in subunit C. Scale dashes are in 1 mm intervals, for reference.

Figure 5: Whole-rock geochemical data from samples at selected stratigraphic heights within the identified subunits (labelled). (a) Total Alkalis-Silica plot for all samples listed in Table 1 (for full data set see Electronic Appendix). Stars indicate bulk samples of subunits (A being lightest blue, B middle blue, C darkest blue). Squares are samples within these units, colour coded by subunit they belong to. (b) shows selected elements changing with stratigraphic height. Black bars indicate the thickness of the region sampled for each whole rock analysis.

Figure 6: Back scattered electron (BSE) images of representative crystals from subunits A – C. No zoning is evident in either the melt inclusion-bearing olivine (a), (b) or the feldspar (c). SIMS spot locations for melt inclusion analyses are evident in (a) and (b). In (a) and (b) the scale bar in 100 µm, in (c) the scale bar is 200 µm.

Figure 7: Phenocryst compositions of feldspar (a) and olivine (b) from the three major subunits identified. Subunit A (circles), subunit B (triangles) and subunit C (squares). For all data see Electronic Appendix.

Figure 8: (a) Matrix glass (crosses) and melt inclusion (filled symbols) compositions from the three main subunits of the ~~compositionally~~ zoned fall. (b-d) melt inclusion compositions and volatile concentrations from all three main subunits of the zoned fall; subunit symbols as in previous figure. (e) Primitive mantle normalised (Sun & McDonough, 1985) trace element diagrams for average matrix glass (dashed) and melt inclusion (solid lines) compositions from the three major subunits. No matrix glass trace element data available for subunit C due to the coarsely microcrystalline nature of the groundmass. Colours as in previous figures. ~~Subunit symbols as in previous figure.~~ For all data see Electronic Appendix.

Figure 9: Histogram of modelled entrapment pressures (using MagmaSat of Ghiorso & Gualda, 2015) for melt inclusions from all three subunits (colours in previous figures) of the ~~compositionally zoned~~zoned fall. For all data see Electronic Appendix.

Figure 10: Matrix glass compositions compared with the compositions of the three dominant crystal phases; subunit symbols as in previous figure. Stage 1 shows fractional crystallisation of plagioclase feldspar and olivine driving the evolution of the matrix glass. Stage 2 highlights the influence of the accumulation of anorthoclase feldspar. Compositions of crystal phases are average compositions from subunit C (plagioclase and olivine), and subunit B (anorthoclase feldspar). For all data see Electronic Appendix.

Formatted: Font: Times New Roman

Formatted: Normal, Line spacing: 1.5 lines

Table 1
Click here to download Table: Table 1.doc

Table 1: Samples of the compositionally-zoned fall

Sample	Stratigraphic height sampled over (in cm from base)	Subunit
AI15-628A	Bulk sample 0 – 80cm	A
AI14-439G	0 – 15cm	A
AI14-439F	15 – 35cm	A
AI14-439E	35 – 50cm	A
AI15-628B	Bulk sample 80 – 120cm	B
AI14-439D	80 – 90cm	B
AI14-439C	90 – 105cm	B
AI14-439B	120 – 130cm	C
AI14-439A	130 – 140cm	C
AI15-628C	Bulk sample 120 – 140cm	C

Table 2: Temperatures and entrapment pressures of the subunits of the compositionally-zoned fall

Sample	Description	Average calculated Fe-Ti Oxide temperature [(1)] *(range)*	Average calculated *f*O2 ΔNNO [(1)] *(range)*	Maximum modelled entrapment pressure [(2)]
AI15-628A	Subunit A- lower	**845 °C** *(841 – 853)*	**-2.28** *(-2.30 – -2.26)*	**250 MPa**
AI15-628B	Subunit B- mid			**240 MPa**
AI15-628C	Subunit C- upper	**866 °C** *(819 – 886)*	**-1.94** *(-2.42– -1.83)*	**216 MPa**

(1) Using Ghiorso & Evans (2008) calibration
(2) Using the MagmaSat App developed from Gualda & Ghiorso (2014)

Figure 1

Click here to download high resolution image

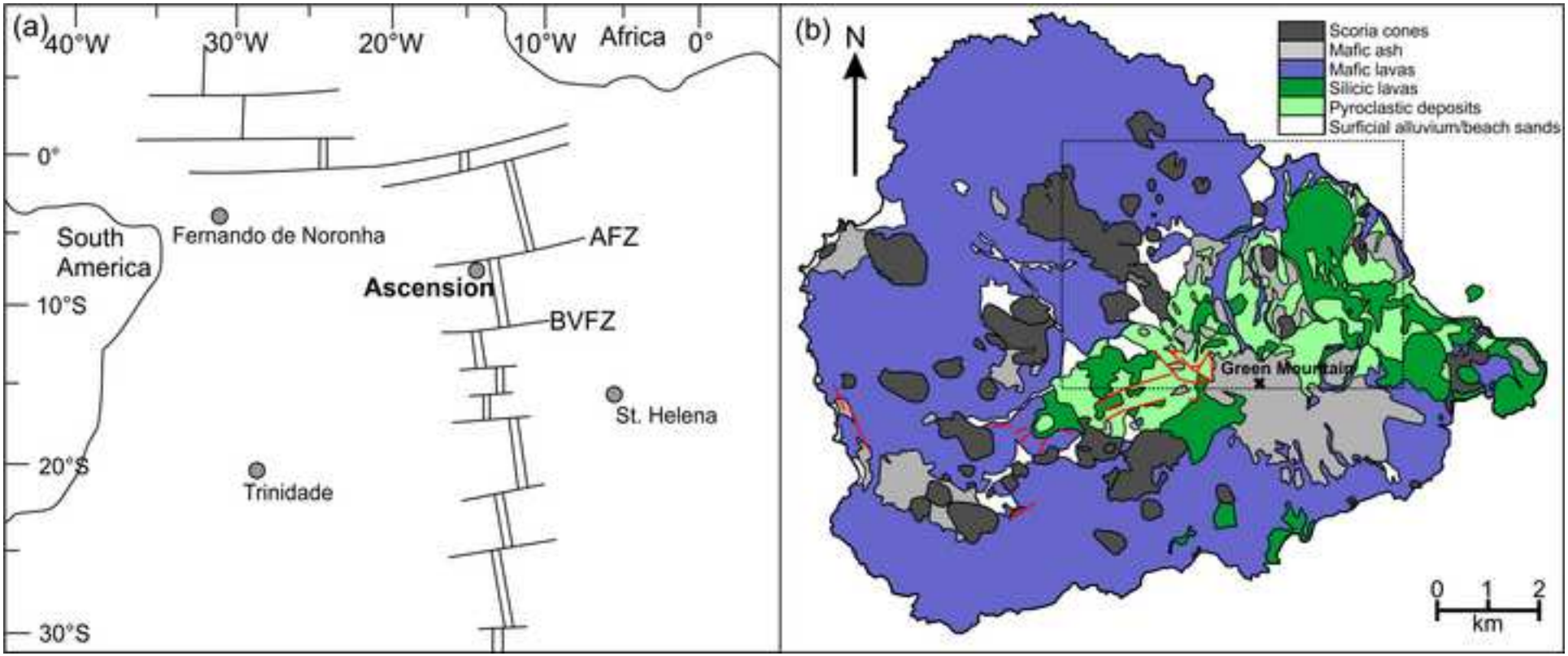

Figure 2

Click here to download high resolution image

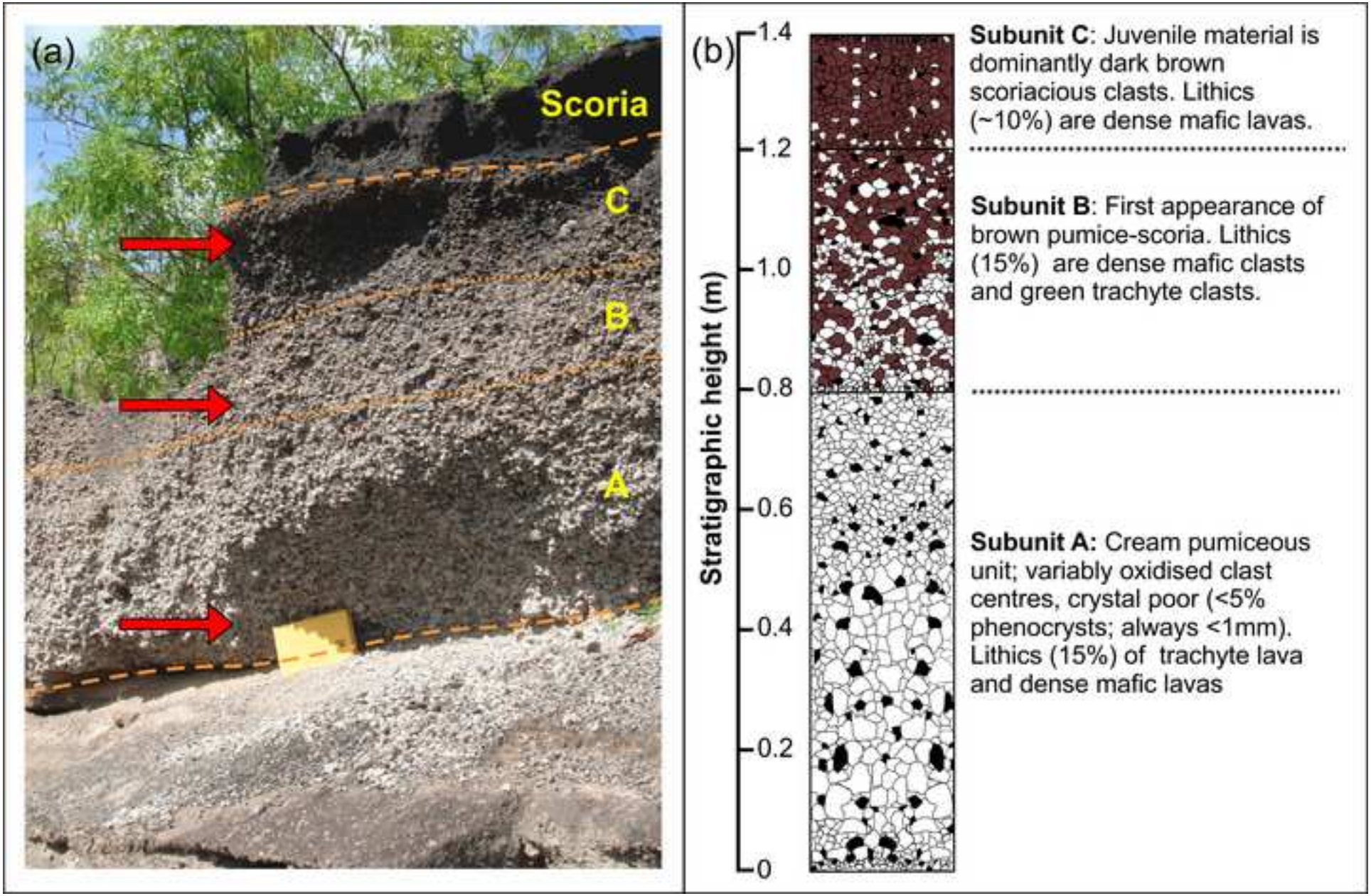

Figure 3

Click here to download high resolution image

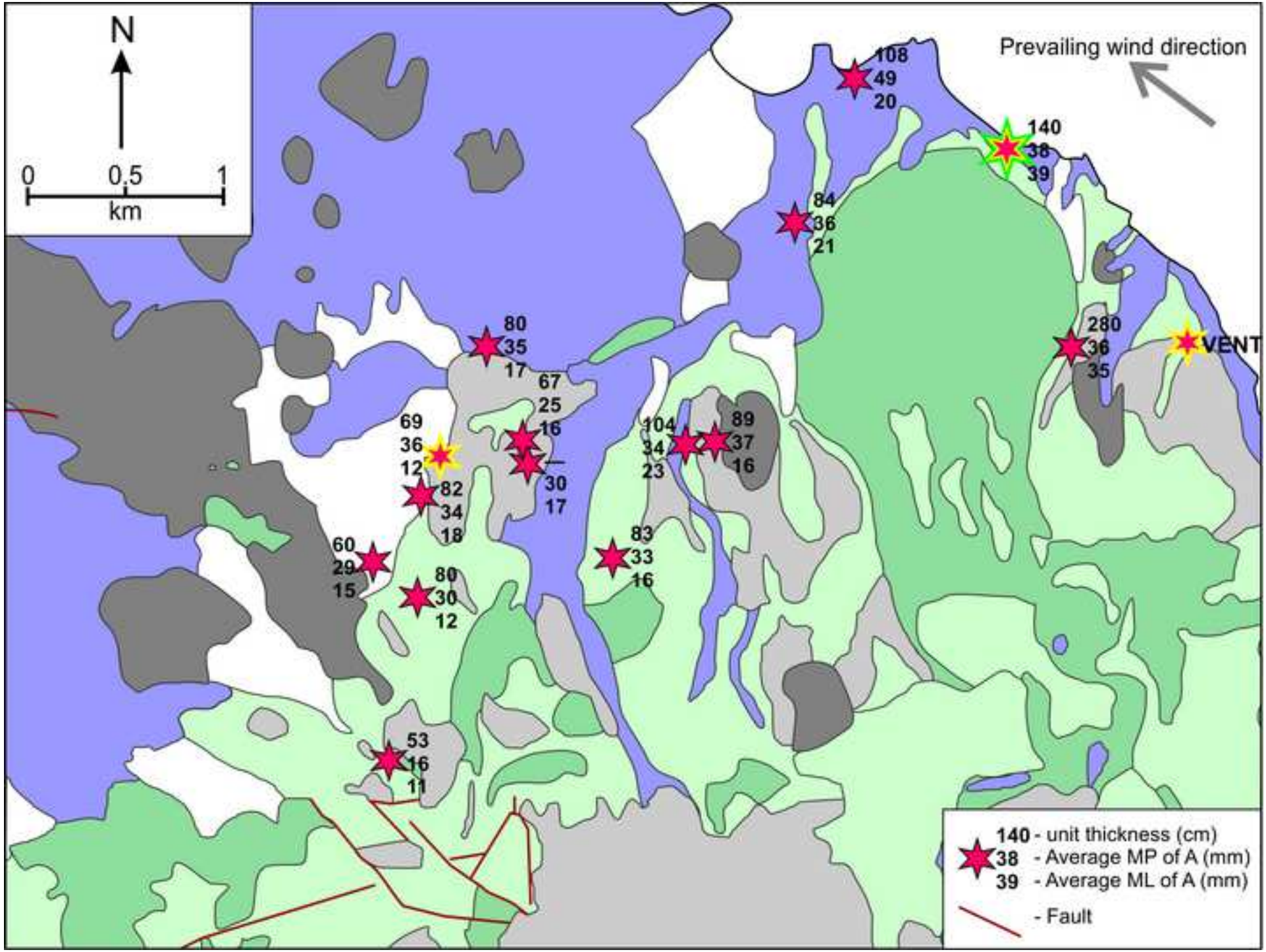

Figure 4

Click here to download high resolution image

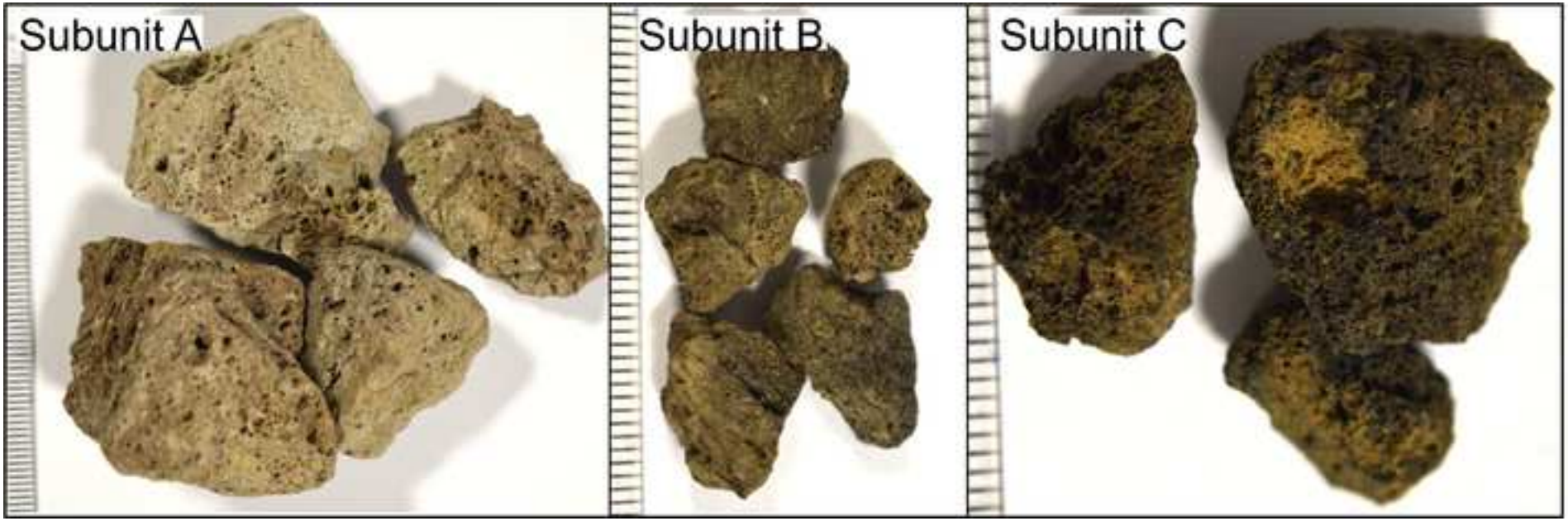

Figure 5

Click here to download high resolution image

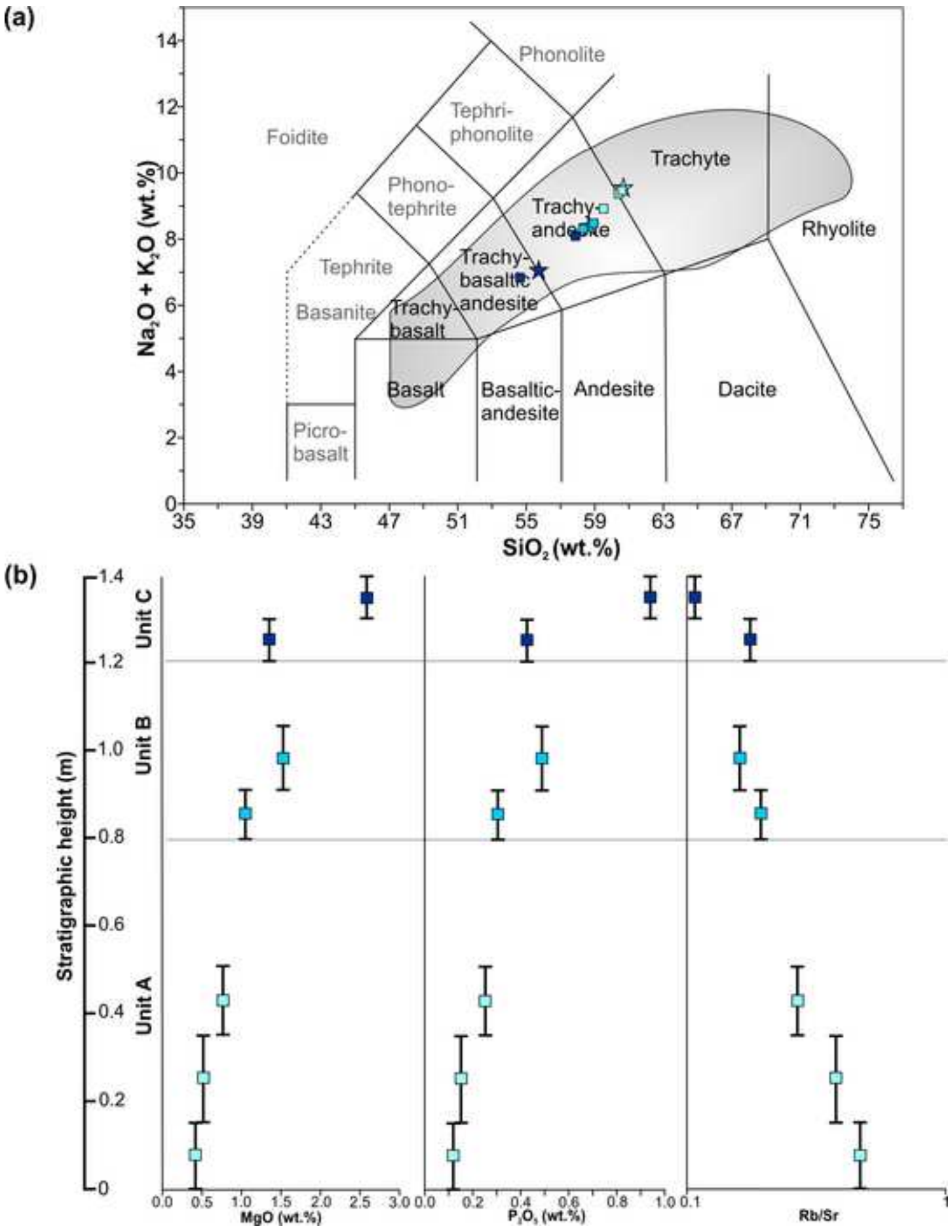

Figure 6

Click here to download high resolution image

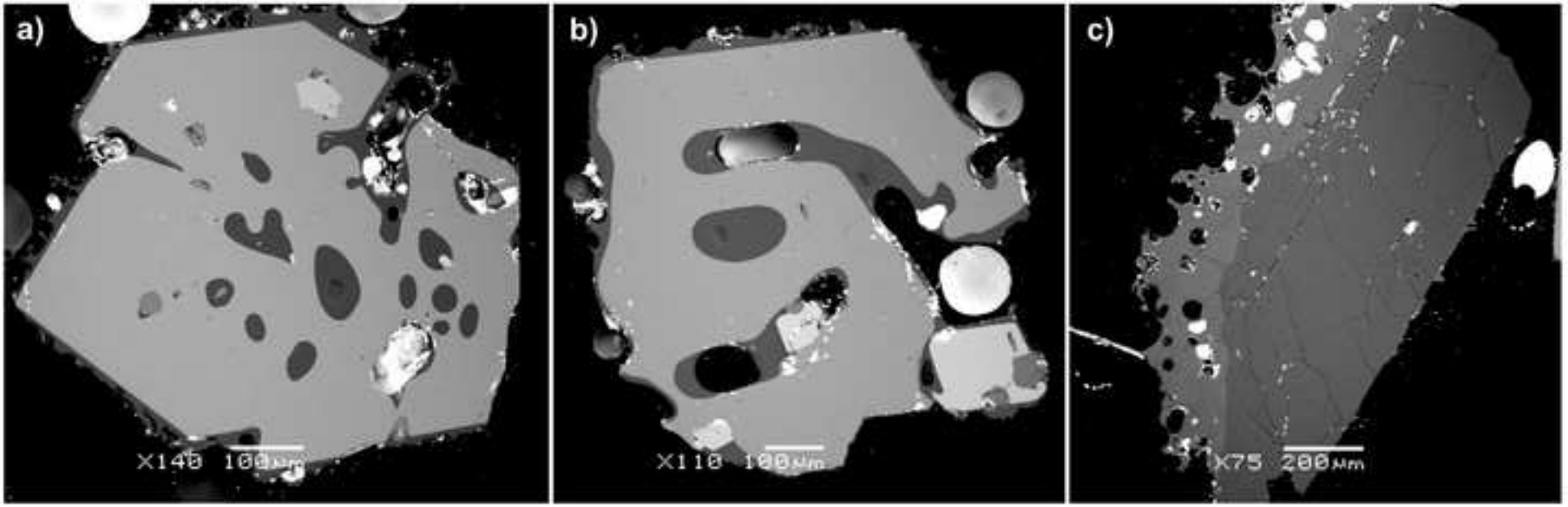

Figure 7

Click here to download high resolution image

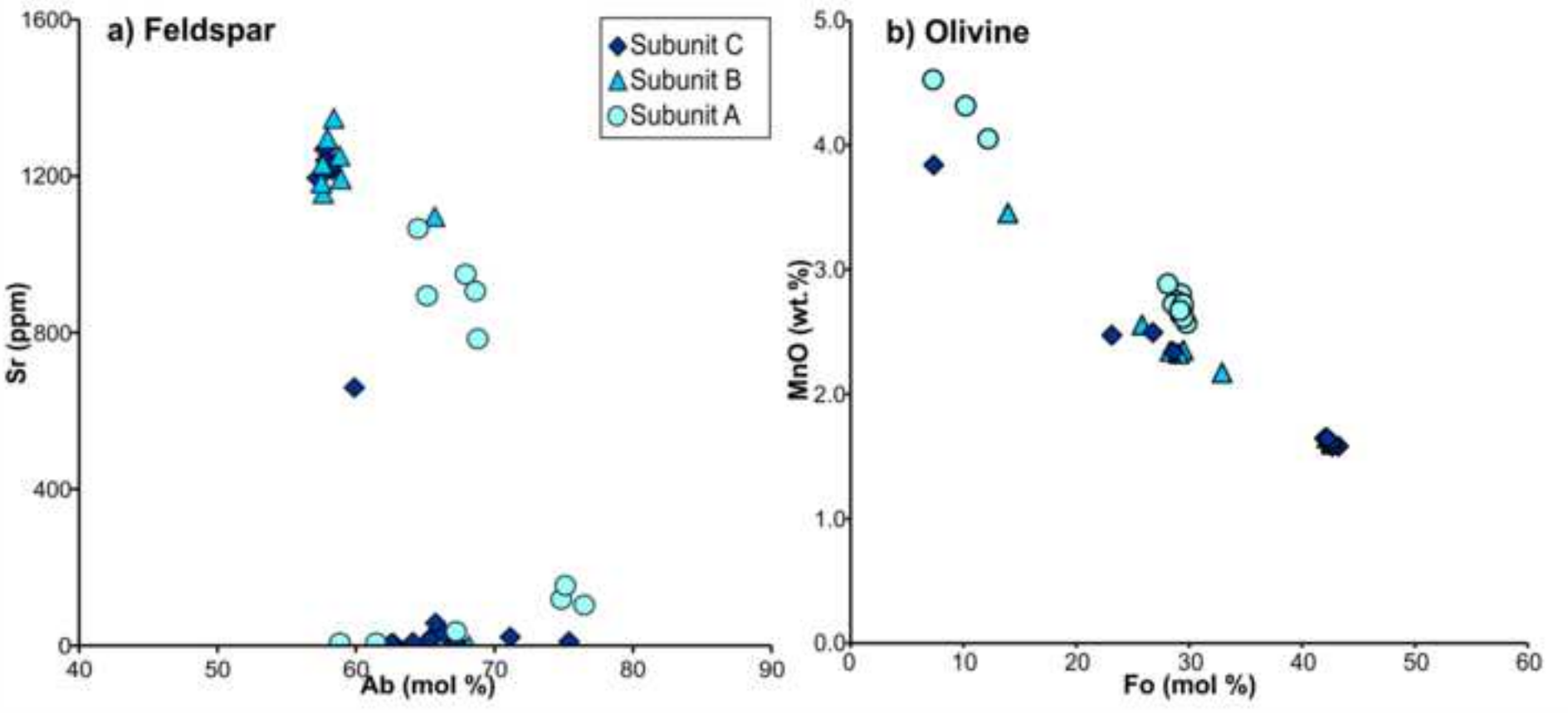

Figure 8

Click here to download high resolution image

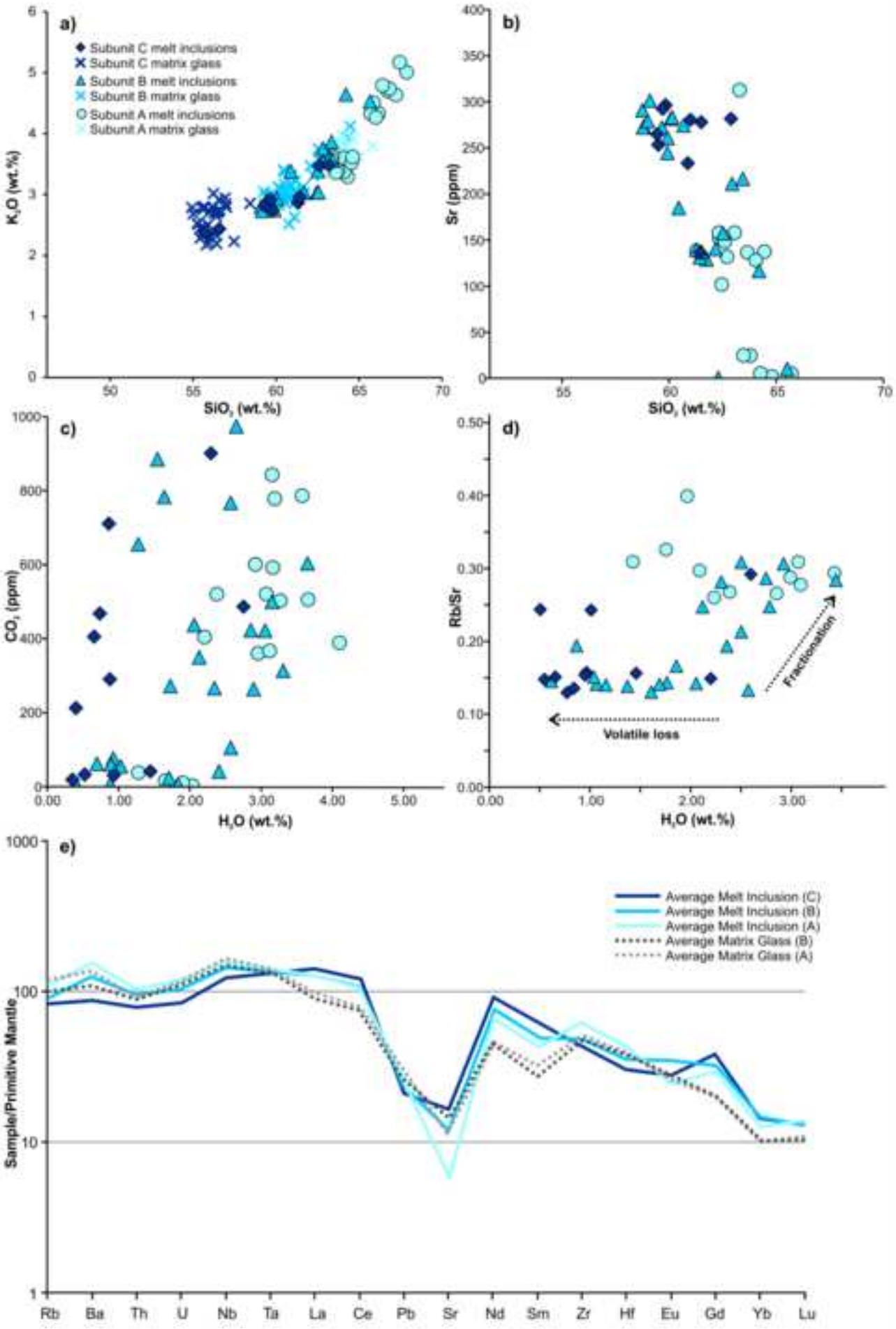

Figure 9

Click here to download high resolution image

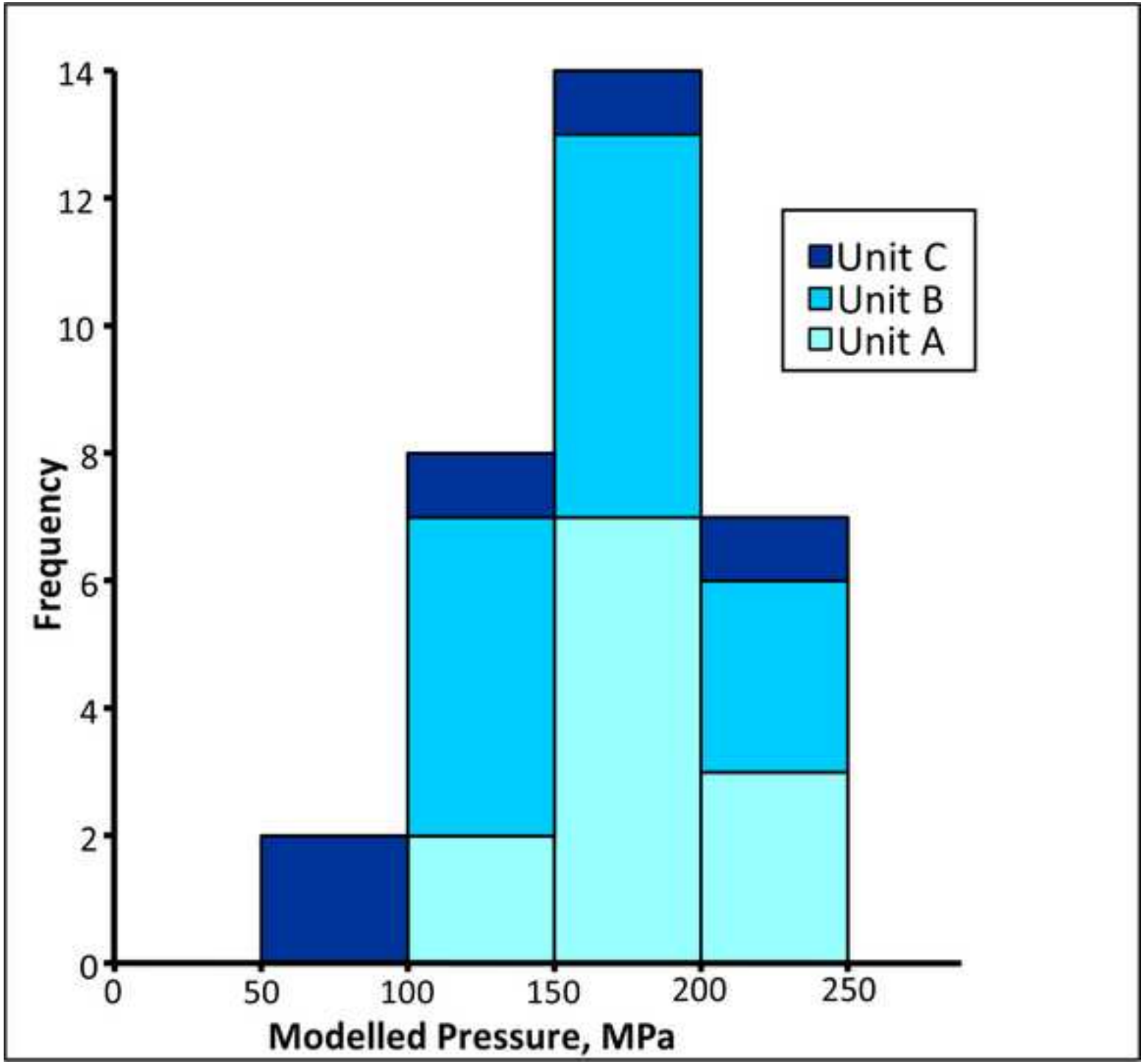

Figure 10

Click here to download high resolution image

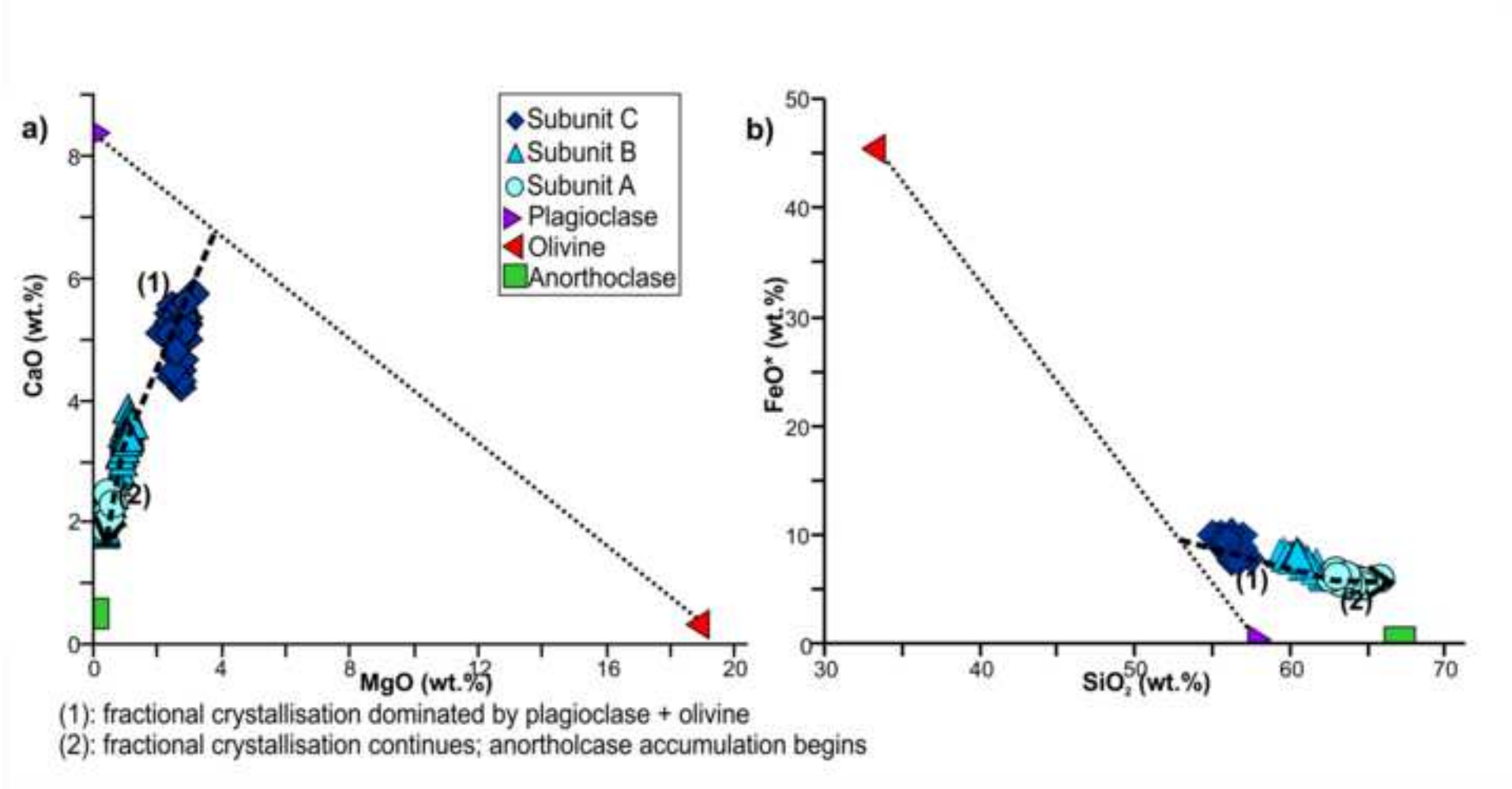

(1): fractional crystallisation dominated by plagioclase + olivine

(2): fractional crystallisation continues; anortholcase accumulation begins

Electronic Supplementary Material (online publication only)

Click here to download Electronic Supplementary Material (online publication only): ElectronicAppendix1.xlsx